

90. Axions and Other Similar Particles

Revised October 2021 by A. Ringwald (DESY, Hamburg), L. J Rosenberg (U. Washington) and G. Rybka (U. Washington).

90.1 Introduction

In this section, we list coupling-strength and mass limits for light neutral scalar or pseudoscalar bosons that couple weakly to normal matter and radiation. Such bosons may arise from the spontaneous breaking of a global U(1) symmetry, resulting in a massless Nambu-Goldstone (NG) boson. If there is a small explicit symmetry breaking, either already in the Lagrangian or due to quantum effects such as anomalies, the boson acquires a mass and is called a pseudo-NG boson. Typical examples are axions (*a*) [1–4] and majorons [5, 6], associated, respectively, with a spontaneously broken Peccei-Quinn and lepton-number symmetry.

A common feature of these light bosons ϕ is that their coupling to Standard-Model particles is suppressed by the energy scale that characterizes the symmetry breaking, *i.e.*, the decay constant f . The interaction Lagrangian is

$$\mathcal{L} = f^{-1} J^\mu \partial_\mu \phi, \quad (90.1)$$

where J^μ is the Noether current of the spontaneously broken global symmetry. If f is very large, these new particles interact very weakly. Detecting them would provide a window to physics far beyond what can be probed at accelerators.

Axions are of particular interest because the Peccei-Quinn (PQ) mechanism remains perhaps the most credible scheme to preserve CP -symmetry in QCD. Moreover, the cold dark matter (CDM) of the Universe may well consist of axions and they are searched for in dedicated experiments with a realistic chance of discovery.

Originally it was assumed that the PQ scale f_a was related to the electroweak symmetry-breaking scale $v_{EW} = (\sqrt{2}G_F)^{-1/2} = 247$ GeV. However, the associated “standard” and “variant” axions were quickly excluded—we refer to the Listings for detailed limits. Here we focus on “invisible axions” with $f_a \gg v_{EW}$ as the main possibility.

Axions have a characteristic two-photon vertex, inherited from their mixing with π^0 and η . This coupling allows for the main search strategy based on axion-photon conversion in external magnetic fields [7], an effect that also can be of astrophysical interest. While for axions the product “ $a\gamma\gamma$ interaction strength \times mass” is essentially fixed by the corresponding π^0 properties, one may consider a more general class of axion-like particles (ALPs) where the two parameters (coupling and mass) are independent. A number of experiments explore this more general parameter space. ALPs populating the latter are predicted to arise generically, in addition to the axion, in low-energy effective field theories emerging from string theory [8–15]. The latter often contain also very light Abelian vector bosons under which the Standard-Model particles are not charged: so-called hidden-sector photons, dark photons or paraphotons. They share a number of phenomenological features with the axion and ALPs, notably the possibility of hidden photon to photon conversion and of hidden photon dark matter [16–18]. Their physics cases and the current constraints are compiled in Refs. [19–22].

90.2 Theory

90.2.1 Peccei-Quinn mechanism and axions

The QCD Lagrangian includes a CP -violating term $\mathcal{L}_\Theta = -\bar{\Theta}(\alpha_s/8\pi) G^{\mu\nu a} \tilde{G}_{\mu\nu}^a$, where $-\pi \leq \bar{\Theta} \leq +\pi$ is the effective Θ parameter after diagonalizing quark masses, $G_{\mu\nu}^a$ is the color field strength tensor, and $\tilde{G}^{a,\mu\nu} \equiv \epsilon^{\mu\nu\lambda\rho} G_{\lambda\rho}^a/2$, with $\varepsilon^{0123} = 1$, its dual. This term induces an electric dipole

moment (EDM) of the neutron of size $d_n = C_{\text{EDM}} e \bar{\Theta}$, where $C_{\text{EDM}} = 2.4(1.0) \times 10^{-16} \text{ cm}$ [23]. Experimental upper bounds on the latter, $|d_n| < 1.8 \times 10^{-26} e \text{ cm}$ [24, 25], imply $|\bar{\Theta}| \lesssim 10^{-10}$ even though $\bar{\Theta} = \mathcal{O}(1)$ is otherwise completely satisfactory. The spontaneously broken global Peccei-Quinn symmetry $U(1)_{\text{PQ}}$ was introduced to solve this “strong CP problem” [1, 2], the axion being the pseudo-NG boson of $U(1)_{\text{PQ}}$ [3, 4]. This symmetry is broken due to the axion’s anomalous triangle coupling to gluons,

$$\mathcal{L} = \left(\frac{a}{f_a} - \bar{\Theta} \right) \frac{\alpha_s}{8\pi} G^{\mu\nu a} \tilde{G}_{\mu\nu}^a, \quad (90.2)$$

where a is the axion field and f_a the axion decay constant. Color anomaly factors have been absorbed in the normalization of f_a which is defined by this Lagrangian. Thus normalized, f_a is the quantity that enters all low-energy phenomena [26]. Non-perturbative topological fluctuations of the gluon fields in QCD induce a potential for a whose minimum is at $a = \bar{\Theta} f_a$, thereby canceling the $\bar{\Theta}$ term in the QCD Lagrangian and thus restoring CP symmetry.

The resulting axion mass, in units of the PQ scale f_a , is identical to the square root of the topological susceptibility in QCD, $m_a f_a = \sqrt{\chi}$. The latter can be evaluated further [27, 28], exploiting the chiral limit (masses of up and down quarks much smaller than the scale of QCD), yielding $m_a f_a = \sqrt{\chi} \approx f_\pi m_\pi$, where $m_\pi = 135 \text{ MeV}$ and $f_\pi \approx 92 \text{ MeV}$. In more detail one finds, by including $\mathcal{O}(\alpha)$ QED corrections and next-to-next-to-leading order (NNLO) corrections in chiral perturbation theory [29],

$$m_a = 5.691(51) \left(\frac{10^9 \text{ GeV}}{f_a} \right) \text{ meV}. \quad (90.3)$$

A direct calculation of the topological susceptibility via QCD lattice simulations finds almost the same central value, albeit with an about five times larger error bar [30].

The axion’s anomalous coupling to gluons induces, at energies below the confinement scale of QCD, a model-independent coupling of the axion to the operator giving rise to the EDM of the nucleon (N),

$$\mathcal{L}_{aN\gamma} = -\frac{i}{2} g_{aN\gamma} a \bar{\Psi}_N \sigma_{\mu\nu} \gamma_5 \Psi_N F^{\mu\nu}, \quad (90.4)$$

where the coupling constants of the neutron (n) and the proton (p) are given by

$$g_{an\gamma} = -g_{ap\gamma} = e \frac{C_{\text{EDM}}}{f_a} = (3.7 \pm 1.5) \times 10^{-3} \left(\frac{1}{f_a} \right) \frac{1}{\text{GeV}}. \quad (90.5)$$

This coupling, as a function of the axion mass, is displayed in Fig. 90.1, where the thickness of the yellow band presents the theoretical uncertainty given in Eq. (90.5).

Axions with $f_a \gg v_{\text{EW}}$ evade almost all current experimental limits. One generic class of models invokes “hadronic axions” where new heavy quarks carry $U(1)_{\text{PQ}}$ charges, leaving ordinary quarks and leptons without tree-level axion couplings. The archetype is the KSVZ model [32, 33], where in addition the heavy new quarks are electrically neutral. Another generic class requires at least two Higgs doublets and ordinary quarks and leptons carry PQ charges, the archetype being the DFSZ model [34, 35]. All of these models contain at least one electroweak singlet scalar that acquires a vacuum expectation value and thereby breaks the PQ symmetry. The KSVZ and DFSZ models are frequently used as benchmark examples, but other models exist where both heavy quarks and Higgs doublets carry PQ charges. In supersymmetric models, the axion is part of a supermultiplet and thus inevitably accompanied by a spin-0 saxion and a spin-1/2 axino, which both also have couplings suppressed by f_a and are expected to have large masses due to supersymmetry breaking [36].

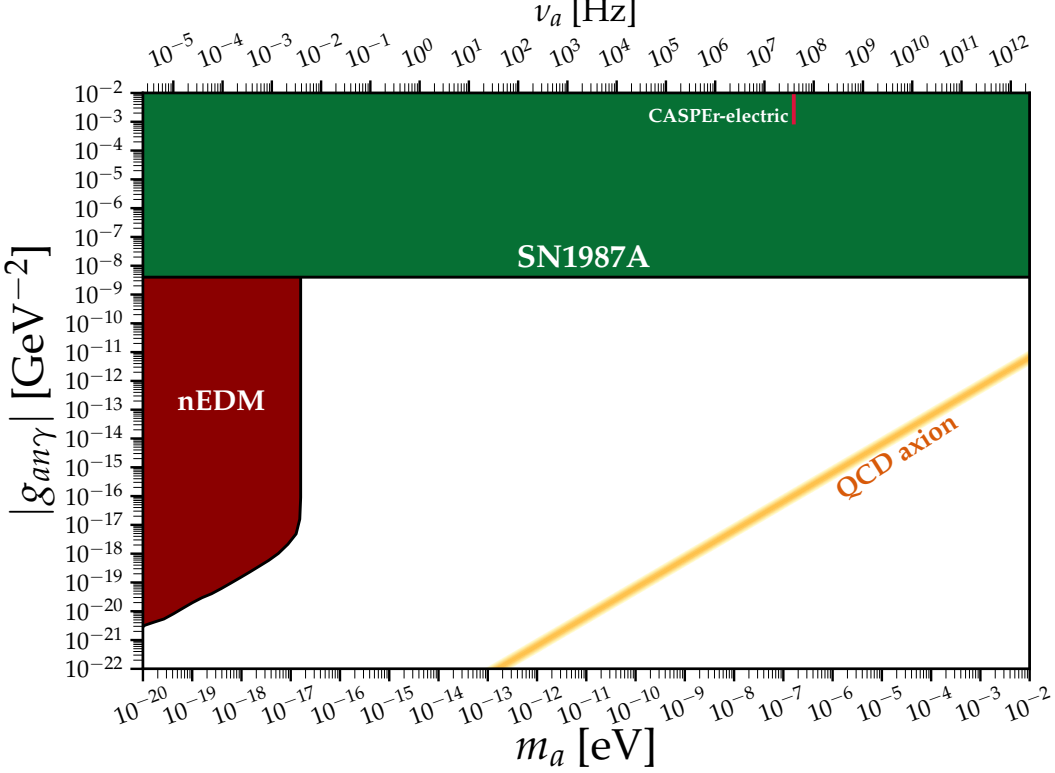


Figure 90.1: Exclusion plot for ALP-EDM coupling as described in the text. Figure courtesy of Ciaran O'Hare [31].

90.2.2 Model-dependent axion couplings

Although the generic axion interactions scale approximately with f_π/f_a from the corresponding π^0 couplings, there are non-negligible model-dependent factors and uncertainties. The axion's two-photon interaction plays a key role for many searches,

$$\mathcal{L}_{a\gamma\gamma} = -\frac{g_{a\gamma\gamma}}{4} a F_{\mu\nu} \tilde{F}^{\mu\nu} = g_{a\gamma\gamma} a \mathbf{E} \cdot \mathbf{B}, \quad (90.6)$$

where F is the electromagnetic field-strength tensor and $\tilde{F}^{\mu\nu} \equiv \epsilon^{\mu\nu\lambda\rho} F_{\lambda\rho}/2$, with $\epsilon^{0123} = 1$, its dual. The coupling constant is [37]

$$g_{a\gamma\gamma} = \frac{\alpha}{2\pi f_a} \left(\frac{E}{N} - 1.92(4) \right) = \left(0.203(3) \frac{E}{N} - 0.39(1) \right) \frac{m_a}{\text{GeV}^2}, \quad (90.7)$$

where E and N are the electromagnetic and color anomalies of the axial current associated with the axion. In grand unified models, and notably for DFSZ [34, 35], $E/N = 8/3$, whereas for KSVZ [32, 33] $E/N = 0$ if the electric charge of the new heavy quark is taken to vanish. In general, a broad range of E/N values is possible [38–41], as indicated by the diagonal yellow band in Fig. 90.2, whose width is roughly determined by the boundary values $E/N = 44/3$ and $E/N = 5/3$, respectively. However, this band still does not exhaust all the possibilities. In fact, there exist classes of QCD axion models whose photon couplings populate the entire still-allowed region outside the yellow band in Fig. 90.2 [42–46], motivating axion search efforts over a wide range of masses and couplings.

The two-photon decay width is

$$\Gamma_{a \rightarrow \gamma\gamma} = \frac{g_{a\gamma\gamma}^2 m_a^3}{64\pi} = 1.1 \times 10^{-24} \text{ s}^{-1} \left(\frac{m_a}{\text{eV}} \right)^5. \quad (90.8)$$

The second expression uses Eq. (90.7) with $E/N = 0$. Axions decay faster than the age of the Universe if $m_a \gtrsim 20$ eV.

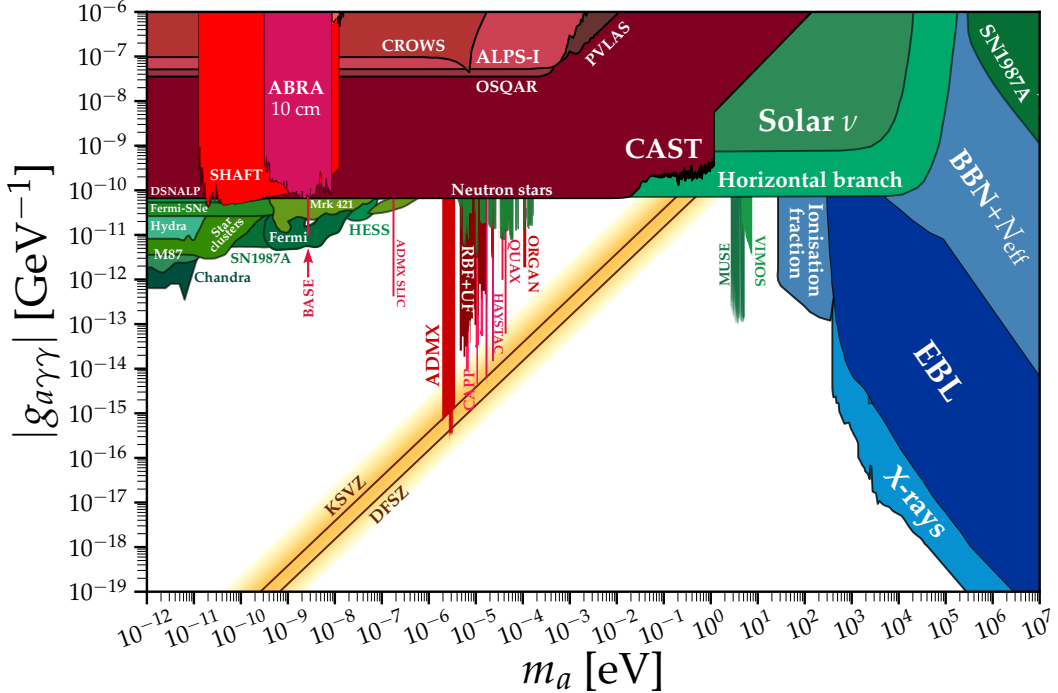


Figure 90.2: Exclusion plot for ALP-photon coupling as described in the text. Figure courtesy of Ciaran O'Hare [31].

The interaction with fermions f has derivative form and is invariant under a shift $a \rightarrow a + a_0$ as behoves a NG boson,

$$\mathcal{L}_{aff} = \frac{C_f}{2f_a} \partial_\mu a \bar{\Psi}_f \gamma^\mu \gamma_5 \Psi_f. \quad (90.9)$$

Here, Ψ_f is the fermion field, m_f its mass, and C_f a model-dependent coefficient. The dimensionless combination $g_{aff} \equiv C_f m_f / f_a$ plays the role of a Yukawa coupling and $\alpha_{aff} \equiv g_{aff}^2 / 4\pi$ of a “fine-structure constant.” The often-used pseudoscalar form $\mathcal{L}_{aff} = -i(C_f m_f / f_a) a \bar{\Psi}_f \gamma_5 \Psi_f$ need not be equivalent to the appropriate derivative structure, for example when two NG bosons are attached to one fermion line as in axion emission by nucleon bremsstrahlung [47–49].

In hadronic axion models, C_e vanishes at tree level, but is then generated radiatively at one loop [50, 51],

$$C_e \simeq \frac{3\alpha^2}{4\pi^2} \left[\frac{E}{N} \log \left(\frac{f_a}{m_e} \right) - 1.92 \log \left(\frac{\Lambda_\chi}{m_e} \right) \right], \quad (90.10)$$

where $\Lambda_\chi \simeq 1$ GeV is the chiral symmetry breaking scale. In the DFSZ model [34, 35], the tree-level coupling coefficient to electrons is [50]

$$C_e = \frac{\sin^2 \beta}{3}, \quad (90.11)$$

where $\tan \beta$ is the ratio of the vacuum expectation values of the two Higgs doublets giving masses to the up- and down-type quarks, respectively: $\tan \beta = v_u/v_d$. The resulting prediction for the axion-electron coupling, as a function of the axion mass, for the KSVZ axion ($E/N = 0$), hadronic axions, with $5/3 \leq E/N \leq 44/3$, and the DFSZ axion is displayed in Fig. 90.3. For the DFSZ range we have taken into account the constraint $0.28 \lesssim \tan \beta \lesssim 140$ [52] arising from the requirement of perturbative unitarity of the Yukawa couplings of Standard Model fermions.

For nucleons, $C_{p,n}$ have been determined as [37]

$$\begin{aligned} C_p &= -0.47(3) + 0.88(3)C_u - 0.39(2)C_d - 0.038(5)C_s \\ &\quad - 0.012(5)C_c - 0.009(2)C_b - 0.0035(4)C_t, \\ C_n &= -0.02(3) + 0.88(3)C_d - 0.39(2)C_u - 0.038(5)C_s \\ &\quad - 0.012(5)C_c - 0.009(2)C_b - 0.0035(4)C_t, \end{aligned} \quad (90.12)$$

in terms of the corresponding model-dependent quark couplings C_q , $q = u, d, s, c, b, t$. For hadronic axions, the latter vanish at tree-level, which means that C_n is expected to be much smaller than C_p . In the DFSZ model, $C_u = C_c = C_t = \frac{1}{3} \cos^2 \beta$ and $C_d = C_s = C_b = \frac{1}{3} \sin^2 \beta$, and C_p and C_n , as functions of β ,

$$\begin{aligned} C_p &= -0.435 \sin^2 \beta + (-0.182 \pm 0.025), \\ C_n &= 0.414 \sin^2 \beta + (-0.160 \pm 0.025), \end{aligned} \quad (90.13)$$

The resulting prediction for the axion-neutron coupling, as a function of the axion mass, for the KSVZ axion and the DFSZ axion is displayed in Fig. 90.4.

The axion-pion interaction is given by the Lagrangian [51]

$$\mathcal{L}_{a\pi} = \frac{C_{a\pi}}{f_\pi f_a} \partial_\mu a \left(\pi^0 \pi^+ \partial_\mu \pi^- + \pi^0 \pi^- \partial_\mu \pi^+ - 2\pi^+ \pi^- \partial_\mu \pi^0 \right), \quad (90.14)$$

where $C_{a\pi} = (1-z)/[3(1+z)]$ in hadronic models and $C_{a\pi} = (1-z)/[3(1+z)] - (1/9) \cos 2\beta$ in the DFSZ model [41], with $z = m_u/m_d = 0.48(3)$ [37].

90.3 Laboratory Searches

90.3.1 Light shining through walls

Searching for “invisible axions” is extremely challenging due to its extraordinarily feeble coupling to normal matter and radiation. Currently, the most promising approaches rely on the axion-two-photon interaction, allowing for axion-photon conversion in external electric or magnetic fields [7]. For the Coulomb field of a charged particle, the conversion is best viewed as a scattering process, $\gamma + Ze \leftrightarrow Ze + a$, called Primakoff effect [53]. In the other extreme of a macroscopic field, usually a large-scale B -field, the momentum transfer is small, the interaction is coherent over a large distance, and the conversion is best viewed as an axion-photon oscillation phenomenon in analogy to neutrino flavor oscillations [54].

Photons propagating through a transverse magnetic field, with incident \mathbf{E}_γ and magnetic field \mathbf{B} parallel, may convert into axions. For $m_a^2 L / 2\omega \ll 2\pi$, where L is the length of the B field region and ω the photon energy, the resultant axion beam is coherent with the incident photon beam and the conversion probability is $\Pi \sim (1/4)(g_{a\gamma\gamma} BL)^2$. A practical realization uses a laser beam propagating down the bore of a superconducting dipole magnet (like the bending magnets in high-energy accelerators). If another magnet is in line with the first, but shielded by an optical barrier, then photons may be regenerated from the pure axion beam [55, 56]. The overall probability is $P(\gamma \rightarrow A \rightarrow \gamma) = \Pi^2$.

The first such Light-Shining-through-Walls (LSW) experiment was performed by the BFRT (Brookhaven-Fermilab-Rochester-Trieste) collaboration. It utilized two magnets of length $L =$

4.4 m and $B = 3.7$ T and found $|g_{a\gamma\gamma}| < 6.7 \times 10^{-7}$ GeV $^{-1}$ at 95% CL for $m_a < 1$ meV [57, 58]. More recently, several such experiments were performed (see Listings) [59–65]. The current best limit, $|g_{a\gamma\gamma}| < 3.5 \times 10^{-8}$ GeV $^{-1}$ at 95% CL for $m_a \lesssim 0.3$ meV (see Fig. 90.2), has been achieved by the OSQAR (Optical Search for QED Vacuum Birefringence, Axions, and Photon Regeneration) experiment, which exploited two 9 T LHC dipole magnets and an 18.5 W continuous wave laser emitting at the wavelength of 532 nm [65]. The ALPS I (Any Light Particle Search I) experiment achieved a similar sensitivity [63], see Fig. 90.2. Some of these experiments have also reported limits for scalar bosons where the photon \mathbf{E}_γ must be chosen perpendicular to the magnetic field \mathbf{B} .

The concept of resonantly enhanced photon regeneration may open unexplored regions of coupling strength [66–68]. In this scheme, both the production and detection magnets are within Fabry-Perot optical cavities and actively locked in frequency. The $\gamma \rightarrow a \rightarrow \gamma$ rate is enhanced by a factor $\mathcal{F}\mathcal{F}'/\pi^2$ relative to a single-pass experiment, where \mathcal{F} and \mathcal{F}' are the finesse of the two cavities. The resonant enhancement could be of order $10^{(10-12)}$, improving the $g_{a\gamma\gamma}$ sensitivity by $10^{(2.5-3)}$. The experiment ALPS II (Any Light Particle Search II) is based on this concept and aims at an improvement of the current laboratory bound on $g_{a\gamma\gamma}$ by a factor $\sim 10^3$ in the year 2022 [69].

Resonantly enhanced photon regeneration has already been exploited in experiments searching for “radiowaves shining through a shielding” [70–73]. For $m_a \lesssim 10^{-5}$ eV, the upper bound on $g_{a\gamma\gamma}$ established by the CROWS (CERN Resonant Weakly Interacting sub-eV Particle Search) experiment [74] is slightly less stringent than the one set by OSQAR, see Fig. 90.2.

90.3.2 Photon polarization

An alternative to regenerating the lost photons is to use the beam itself to detect conversion: the polarization of light propagating through a transverse B field suffers dichroism and birefringence [75]. Dichroism: The E_\parallel component, but not E_\perp , is depleted by axion production, causing a small rotation of linearly polarized light. For $m_a^2 L / 2\omega \ll 2\pi$, the effect is independent of m_a . For heavier axions, it oscillates and diminishes as m_a increases, and it vanishes for $m_a > \omega$. Birefringence: This effect occurs because there is mixing of virtual axions in the E_\parallel state, but not for E_\perp . Hence, linearly polarized light will develop elliptical polarization. Higher-order QED also induces vacuum magnetic birefringence (VMB). A search for these effects was performed in the same dipole magnets of the BFRT experiment mentioned before [76]. The dichroic rotation gave a stronger limit than the ellipticity rotation: $|g_{a\gamma\gamma}| < 3.6 \times 10^{-7}$ GeV $^{-1}$ at 95% CL, for $m_a < 5 \times 10^{-4}$ eV. The ellipticity limits are better at higher masses, as they fall off smoothly and do not terminate at m_a .

In 2006, the PVLAS collaboration reported a signature of magnetically induced vacuum dichroism that could be interpreted as the effect of a pseudoscalar with $m_a = 1\text{--}1.5$ meV and $|g_{a\gamma\gamma}| = (1.6\text{--}5) \times 10^{-6}$ GeV $^{-1}$ [77]. Later, it turned out that these findings are due to instrumental artifacts [78]. This particle interpretation is also excluded by the above photon regeneration searches that were inspired by the original PVLAS result. The fourth generation setup of the PVLAS experiment has published results on searches for VMB (see Fig. 90.2) and dichroism [79]. The bounds from the non-observation of the latter on $g_{a\gamma\gamma}$ are slightly weaker than the ones from OSQAR.

90.3.3 Long-range forces

New bosons would mediate long-range forces, which are severely constrained by “fifth force” experiments [80]. Those looking for new mass-spin couplings provide significant constraints on pseudoscalar bosons [81–86], see for example in Fig. 90.4 the limit on the axion-neutron coupling [87] from torsion balance tests of the gravitational inverse square law [88]. Presently, the most restrictive limits are obtained from combining long-range force measurements with stellar cooling arguments [89, 90]. For the moment, any of these limits are far from realistic values expected for

the QCD axion. Still, these efforts provide constraints on more general low-mass bosons.

In Ref. [91], a method was proposed that can extend the search for axion-mediated spin-dependent forces by several orders of magnitude. By combining techniques used in nuclear magnetic resonance and short-distance tests of gravity, this method appears to be sensitive to the QCD axion in the $\mu\text{eV} - \text{meV}$ mass range, independent of the cosmic axion abundance, if axions have a CP -violating interaction with nuclei as large as the current experimental bound on the electric dipole moment of the neutron allows. The ARIADNE (Axion Resonant InterAction DetectioN Experiment) is under development and employs this approach to search for axion-mediated spin-dependent short-range interactions between a hyper-polarized ^3He sample and an unpolarized tungsten source mas [92]. The method relies on superconducting magnetic shielding to screen the sample from ordinary magnetic field noise. Experimental tests to demonstrate the requirements of ARIADNE, including characterization of the magnetic field backgrounds, are under way [93, 94].

90.4 Axions from Astrophysical Sources

90.4.1 Stellar energy-loss limits

Low-mass weakly-interacting particles (neutrinos, gravitons, axions, baryonic or leptonic gauge bosons, *etc.*) are produced in hot astrophysical plasma, and can thus transport energy out of stars. The coupling strength of these particles with normal matter and radiation is bounded by the constraint that stellar lifetimes or energy-loss rates are not in conflict with observation [95, 96].

We begin this discussion with our Sun and concentrate first on hadronic axions. They are produced predominantly by the Primakoff process $\gamma + Ze \rightarrow Ze + a$. Integrating over a standard solar model yields the axion luminosity [97]

$$L_a = g_{10}^2 \times 1.85 \times 10^{-3} L_\odot, \quad (90.15)$$

where $g_{10} = |g_{a\gamma\gamma}| \times 10^{10} \text{ GeV}$. The maximum of the spectrum is at 3.0 keV, the average at 4.2 keV, and the number flux at Earth is $g_{10}^2 \times 3.75 \times 10^{11} \text{ cm}^{-2} \text{ s}^{-1}$. The solar photon luminosity is fixed, so energy losses due to the Primakoff process require enhanced nuclear energy production and thus enhanced neutrino fluxes. The all-flavor measurements by SNO (Sudbury Neutrino Observatory), together with a standard solar model, imply $L_a \lesssim 0.10 L_\odot$, corresponding to $g_{10} \lesssim 7$ [98], mildly superseding a similar limit from helioseismology (sound speed, surface helium and convective radius) [99]. In Ref. [100], this limit was improved to $g_{10} < 4.1$ (at 3σ), see Fig. 90.2, exploiting a new statistical analysis that combined helioseismology and solar neutrino observations, including theoretical and observational errors, and accounting for tensions between input parameters of solar models, in particular the solar element abundances. Going beyond the hadronic axion, Ref. [98] considered also a non-zero axion-electron coupling and obtained the bound on the latter displayed in Fig. 90.3.

A more restrictive limit derives from globular-cluster (GC) stars that allow for detailed tests of stellar-evolution theory. The stars on the horizontal branch (HB) in the color-magnitude diagram have reached helium burning with a core-averaged energy release of about $80 \text{ erg g}^{-1} \text{ s}^{-1}$, compared to Primakoff axion losses of $g_{10}^2 30 \text{ erg g}^{-1} \text{ s}^{-1}$. The accelerated consumption of helium reduces the HB lifetime by about $80/(80 + 30 g_{10}^2)$. Number counts of HB stars in a large sample of 39 Galactic GCs compared with the number of red giants (that are not much affected by Primakoff losses) give a weak indication of non-standard losses which may be accounted by Primakoff-like axion emission, if the photon coupling is in the range $|g_{a\gamma\gamma}| = (2.9 \pm 1.8) \times 10^{-11} \text{ GeV}^{-1}$ [101, 102]. Still, the upper bound found in this analysis,

$$|g_{a\gamma\gamma}| < 6.6 \times 10^{-11} \text{ GeV}^{-1} \text{ (95\% CL)}, \quad (90.16)$$

represents the strongest limit on $g_{a\gamma\gamma}$ for a wide mass range, see Fig. 90.2. The conservative constraint, Eq. (90.16), on $g_{a\gamma\gamma}$ may be translated to $f_a > 3.4 \times 10^7 \text{ GeV}$ ($m_a < 0.2 \text{ eV}$), using

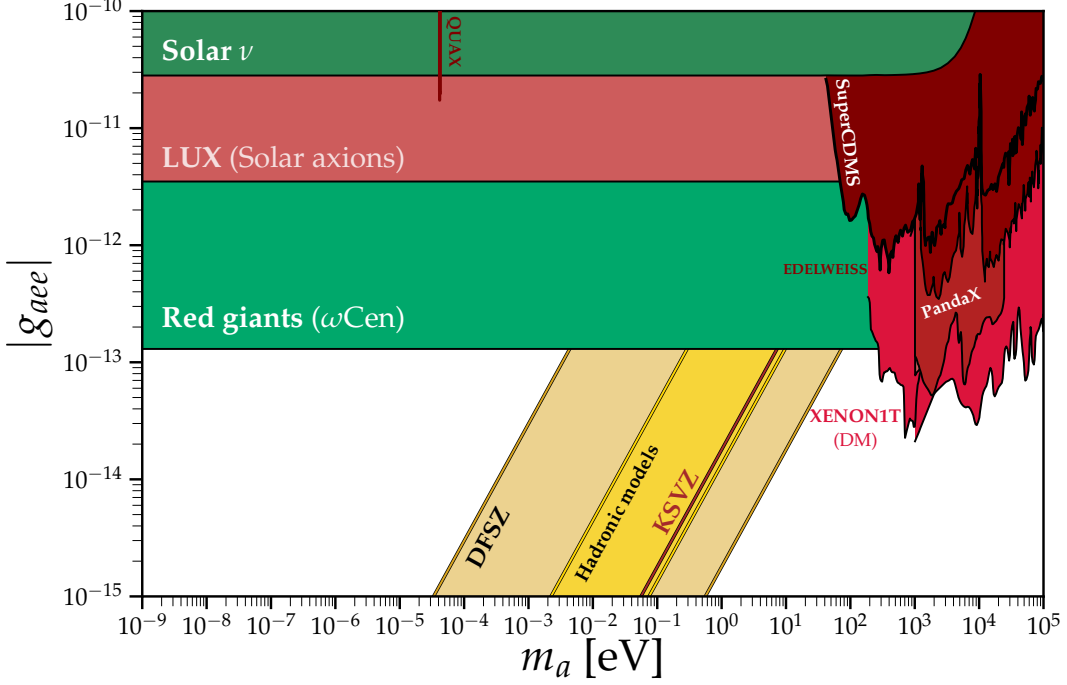


Figure 90.3: Exclusion plot for ALP-electron coupling as described in the text. Figure courtesy of Ciaran O'Hare [31].

$E/N = 0$ as in the KSVZ model, or to $f_a > 1.3 \times 10^7$ GeV ($m_a < 0.5$ eV), for the DFSZ axion model, with $E/N = 8/3$, see Fig. 90.2.

If axions couple directly to electrons, the dominant emission processes are atomic axio-recombination and axio-deexcitation, axio-bremsstrahlung in electron-ion or electron-electron collisions, and Compton scattering [103]. Stars in the red giant (RG) branch of the color-magnitude diagram of GCs are particularly sensitive to these processes: they would lead to an extension of the latter to larger brightness. In fact, the RG branch tip – the brightest point of the RG branch – provides the currently most sensitive method to test the axion coupling to electrons. The strongest bounds on it are derived from analyses of the RG branch tip in several globular clusters [104] and in the Galactic globular cluster ω Centauri [105]. The two analyses lead to very similar results,

$$|g_{aee}| < 1.48 \times 10^{-13} \text{ (95\% CL)} \quad \text{and} \quad |g_{aee}| < 1.3 \times 10^{-13} \text{ (95\% CL)}, \quad (90.17)$$

respectively, see Fig. 90.3. Reference [104] finds also a small hint for extra cooling, corresponding to $|g_{aee}| = 0.60^{+0.32}_{-0.58} \times 10^{-13}$, while Ref. [105] does not find any evidence for exotic cooling.

Bremsstrahlung is also efficient in white dwarfs (WDs), where the Primakoff and Compton processes are suppressed by the large plasma frequency. A comparison of the predicted and observed luminosity function of WDs can be used to put limits on $|g_{aee}|$ [106, 107]. An analysis based on detailed WD cooling treatment and data on the WD luminosity function (WDLF) of the Galactic disk found that electron couplings above $|g_{aee}| \gtrsim 3 \times 10^{-13}$ are disfavoured [108]. Lower couplings cannot be discarded from the current knowledge of the WDLF of the Galactic disk. On the contrary, features in some WDLFs can be interpreted as suggestions for electron couplings in the range $7.2 \times 10^{-14} \lesssim |g_{aee}| \lesssim 2.2 \times 10^{-13}$ [108–110]. This hypothesis will be further scrutinized by the Large Synoptic Survey Telescope (LSST) which is expected to increase the sample of WDs in the Galactic halo to hundreds of thousands [111]. This will allow for the determination of

independent WDLFs from different Galactic populations, greatly reducing the uncertainties related to star formation histories. For pulsationally unstable WDs (ZZ Ceti stars), the period decrease \dot{P}/P is a measure of the cooling speed. The corresponding observations of a handful pulsating WDs imply additional cooling that can be interpreted also in terms of similar axion losses [112–115]. In fact, the combined analysis of these observations gives a good fit for $|g_{aee}| = 2.9 \times 10^{-13}$ and favours the axion (or ALP) interpretation at slightly more than 2σ [41].

Intriguingly, a 3σ preference for the existence of the axion (or an ALP) is found if one combines the hints of excessive cooling of HB stars, RGs and WDs and allows for both a photon and electron coupling [116]. The best fit is obtained for $|g_{a\gamma\gamma}| \sim 1.4 \times 10^{-11} \text{ GeV}^{-1}$ and $|g_{aee}| \sim 1.5 \times 10^{-13}$, respectively, where the photon coupling is compatible with zero at 1σ , whereas the electron coupling is non-zero at the level of 3σ [41, 116].

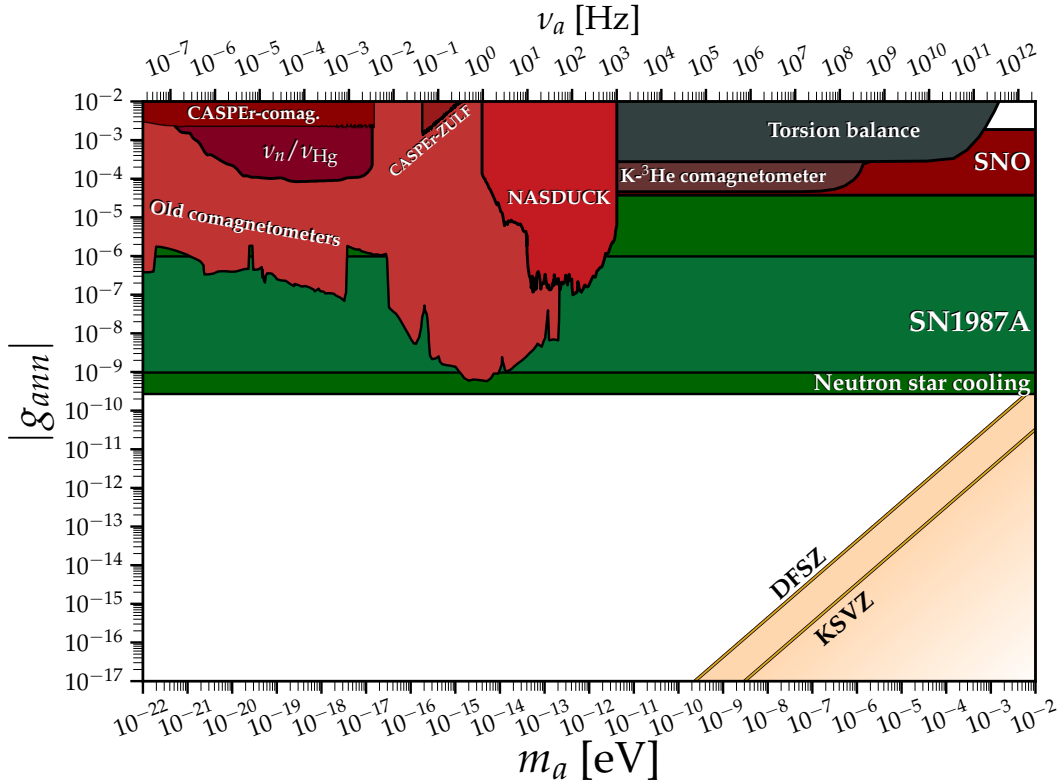


Figure 90.4: Exclusion plot for ALP-neutron coupling as described in the text. Figure courtesy of Ciaran O’Hare [31].

Analogous constraints derive from the measured duration of the neutrino signal of the supernova SN 1987A. Numerical simulations for a variety of cases, including axions and Kaluza-Klein gravitons, reveal that the energy-loss rate of a nuclear medium at the density $3 \times 10^{14} \text{ g cm}^{-3}$ and temperature 30 MeV should not exceed about $1 \times 10^{19} \text{ erg g}^{-1} \text{ s}^{-1}$ [117]. The energy-loss rate from nucleon bremsstrahlung, $N + N \rightarrow N + N + a$, is $(C_N/2f_a)^2(T^4/\pi^2 m_N) F$. Here F is a numerical factor that represents an integral over the dynamical spin-density structure function because axions couple to the nucleon spin. For realistic conditions, even after considerable effort, one is limited to a heuristic estimate leading to $F \approx 1$ [96]. The SN 1987A limits are of particular interest for hadronic axions where the bounds on $|g_{aee}|$ are moot. Using a proton fraction of 0.3, $g_{ann} = 0$, $F = 1$, and $T = 30 \text{ MeV}$, one finds $f_a > 4 \times 10^8 \text{ GeV}$ and $m_a < 16 \text{ meV}$ [96]. A more detailed

numerical calculation [118] with state of the art SN models, again assuming $g_{ann} = 0$, found that a coupling larger than $|g_{app}| \gtrsim 6 \times 10^{-10}$, would shorten significantly the timescale of the neutrino emission. This result is, not surprisingly, rather close to the estimate in Ref. [96]. Improving the calculation of axion emission via nucleon-nucleon bremsstrahlung beyond the basic one-pion exchange approximation appears to loosen the bound [119, 120]. The latter analysis finds a reduction of the axion emissivity by an order of magnitude if one takes into account the non-vanishing mass of the exchanged pion, the contribution from two-pion exchange, effective in-medium nucleon masses and multiple nucleon scattering, leading to a looser bound

$$g_{ann}^2 + 0.61 g_{app}^2 + 0.53 g_{ann} g_{app} < 8.26 \times 10^{-19}, \quad (90.18)$$

see Fig. 90.4. This analysis, however, still neglects another very efficient mechanism for axion production in a SN: the pion production process, $\pi^- + p \rightarrow a + n$, also induced by the axion coupling to nucleons. Pion production was recognized long ago as being competitive with nucleon bremsstrahlung [121–123]. However, only recently it was shown that the pion abundance in the early stages of a SN is much larger than previously expected [124]. Although a complete study of the SN evolution which includes pions self-consistently does not exist at the moment, it was shown in Ref. [125] that pion induced processes dominate over bremsstrahlung and so strengthen the bound on the axion-nucleon coupling. In any case, with the present understanding of SNe (current lack of self-consistent 3D SN simulations) and the sparse data from SN 1987A, the constraint on the axion-nucleon couplings from SN 1987A should be considered more as indicative than as a sharp bound [118].

If axions interact sufficiently strongly they are trapped. Only about three orders of magnitude in g_{aNN} , where $N = n, p$, or m_a are excluded, see Fig. 90.4. For even larger couplings, the axion flux would have been negligible, yet it would have triggered additional events in the detectors, excluding a further range [126]. A possible gap between these two SN 1987A arguments was discussed as the “hadronic axion window” under the assumption that $g_{a\gamma\gamma}$ was anomalously small [127]. This range is now excluded by hot dark matter (HDM) bounds (see below).

Further bounds on the axion-nucleon coupling can be derived from observations of the cooling of neutron stars, in particular the neutron star (NS) in the supernova remnant Cassiopeia A (Cas A). Its surface temperature measured over 10 years reveals an unusually fast cooling rate. This rapid cooling of the Cas A NS may be explained by NS minimal cooling with neutron superfluidity and proton superconductivity [128, 129]. The rapid cooling may also arise from a phase transition of the neutron condensate into a multicomponent state [130]. Recently, Ref. [131] analyzed Cas A NS cooling in the presence of axion emission and obtained

$$g_{app}^2 + 1.6g_{ann}^2 < 1 \times 10^{-18}, \quad (90.19)$$

which is comparable to the SN 1987A bound. Refs. [132, 133] put a less stringent bound on a KSVZ type axion, without an attempt to fit a transient behavior of Cas A,

$$f_a > (5 - 10) \times 10^7 \text{ GeV} \text{ (or } g_{app}^2 < (1 - 6) \times 10^{-17}), \quad (90.20)$$

from the temperatures of Cas A and other NSs. This limit has been confirmed very recently by Ref. [134] focussing again on the CasA NS and finding $f_a > 3 \times 10^7 \text{ GeV}$ (KSVZ) and $f_a > 4.5 \times 10^8 \text{ GeV}$ (DFSZ). The Cas A NS cooling may also be interpreted as a hint for extra cooling caused by the emission of axions from the breaking and re-formation of neutron triplet Cooper pairs [135], requiring a coupling to the neutron of

$$g_{ann}^2 = (1.4 \pm 0.5) \times 10^{-19}, \quad (90.21)$$

corresponding to an axion mass

$$m_a = (2.3 \pm 0.4) \text{ meV}/C_n. \quad (90.22)$$

However, the astrophysical versus instrumental origin of the observed cooling of the CasA NS is still being debated [136]. On the other hand, Ref. [137] considered another hot young NS in the supernova remnant HESS J1731-347. Its high temperature implies that all the neutrino emission processes except neutron-neutron bremsstrahlung must be strongly suppressed, which can be realized with a negligible neutron triplet gap and a large proton singlet gap. In this setup, the bremsstrahlung from neutrons is the dominant channel for axion emission, from which one obtains a limit

$$g_{ann}^2 < 7.7 \times 10^{-20}, \quad (90.23)$$

see Fig. 90.4.

The model-independent axion coupling to the nucleon EDMs, Eq. (90.5), can also be constrained by the non-observation of excess cooling from SN 1987A. Reference [138] presents a determination of the cooling rate due to the axion production process $N + \gamma \rightarrow N + a$, leading to the bound

$$|g_{aN\gamma}| < 4 \times 10^{-9} \text{ GeV}^{-2}, \quad (90.24)$$

see Fig. 90.1.

Finally, let us note that if the interpretation of the various hints for additional cooling of stars, reported in this section in terms of emission of axions with $m_a \sim \text{meV}$, were correct, SNe would lose a large fraction of their energy as axions. This would lead to a diffuse SN axion background in the Universe with an energy density comparable to the extra-galactic background light [139]. However, there is no apparent way of detecting it or the axion burst from the next nearby SN. On the other hand, neutrino detectors such as IceCube, Super-Kamiokande or a future mega-ton water Cherenkov detector will probe exactly the mass region of interest by measuring the neutrino pulse duration of the next Galactic SN [118].

90.4.2 Searches for solar axions and ALPs

Instead of using stellar energy losses to derive axion limits, one can also search directly for these fluxes, notably from the Sun. The main focus has been on ALPs with a two-photon vertex. They are produced by the Primakoff process with a flux given by Eq. (90.15) and an average energy of 4.2 keV, and can be detected at Earth with the reverse process in a macroscopic B -field (“axion helioscope”) [7]. In order to extend the sensitivity in mass towards larger values, one can endow the photon with an effective mass in a gas, $m_\gamma = \omega_{\text{plas}}$, thus matching the axion and photon dispersion relations [140].

An early implementation of these ideas used a conventional dipole magnet, with a conversion volume of variable-pressure gas with a xenon proportional chamber as x-ray detector [141]. The conversion magnet was fixed in orientation and collected data for about 1000 s/day. Axions were excluded for $|g_{a\gamma\gamma}| < 3.6 \times 10^{-9} \text{ GeV}^{-1}$ for $m_a < 0.03 \text{ eV}$, and $|g_{a\gamma\gamma}| < 7.7 \times 10^{-9} \text{ GeV}^{-1}$ for $0.03 < m_a < 0.11 \text{ eV}$ at 95% CL.

Later, the Tokyo axion helioscope used a superconducting magnet on a tracking mount, viewing the Sun continuously. They reported $|g_{a\gamma\gamma}| < 6 \times 10^{-10} \text{ GeV}^{-1}$ for $m_a < 0.3 \text{ eV}$ [142, 143]. This experiment was recommissioned and a similar limit for masses around 1 eV was reported [144].

The most recent helioscope CAST (CERN Axion Solar Telescope) uses a decommissioned LHC dipole magnet on a tracking mount. The hardware includes grazing-incidence x-ray optics with solid-state x-ray detectors, as well as novel x-ray Micromegas position-sensitive gaseous detectors. Exploiting an IAXO (see below) pathfinder system, CAST has established the limit

$$|g_{a\gamma\gamma}| < 6.6 \times 10^{-11} \text{ GeV}^{-1} \quad (95\% \text{ CL}), \quad (90.25)$$

for $m_a < 0.02$ eV [145]. To cover larger masses, the magnet bores are filled with a gas at varying pressure. The runs with ^4He cover masses up to about 0.4 eV [146], providing the ^4He limits shown in Fig. 90.2. To cover yet larger masses, ^3He was used to achieve a larger pressure at cryogenic temperatures. Limits up to 1.17 eV allowed CAST to “cross the axion line” for the KSVZ model [147–149], see Fig. 90.2.

Going to yet larger masses in a helioscope search is not well motivated because of the cosmic HDM bound of $m_a \lesssim 1$ eV (see below). Sensitivity to significantly smaller values of $g_{a\gamma\gamma}$ can be achieved with a next-generation axion helioscope with a much larger magnetic-field cross section. Realistic design options for this “International Axion Observatory” (IAXO) have been studied in some detail [150] and its physics potential has been reviewed recently [151]. Such a next-generation axion helioscope may also push the sensitivity in the product of couplings to photons and to electrons, $g_{a\gamma\gamma}g_{aee}$, into a range beyond stellar energy-loss limits and test the hypothesis that WD, RG, and HB cooling is dominated by axion emission [152, 153]. As a first step towards IAXO, an intermediate experimental stage called BabyIAXO is currently under preparation at DESY [154].

Other Primakoff searches for solar axions and ALPs have been carried out using crystal detectors, exploiting the coherent conversion of axions into photons when the axion angle of incidence satisfies a Bragg condition with a crystal plane [155–159]. However, none of these limits is more restrictive than the one derived from the constraint on the solar axion luminosity ($L_a \lesssim 0.10 L_\odot$) discussed earlier.

Direct detection experiments searching for dark matter (DM) consisting of weakly interacting massive particles have also the capability to search for solar axions and ALPs. For low masses, $m_a \lesssim 100$ eV, the LUX experiment [160] has provided the most stringent bound among those experiments on the axion-electron coupling constant,

$$|g_{aee}| < 3.5 \times 10^{-12} \quad (90\% \text{ CL}), \quad (90.26)$$

see Fig. 90.3, by exploiting the axio-electric effect in liquid xenon. A slightly less stringent limit was set by PandaX-II [161]. However, as obvious from the same figure, this technique has not reached the sensitivity of energy-loss considerations in stars. Recently, the XENON1T collaboration has reported an excess in low energy electronic recoil data peaking around 2-3 keV [162]. A possible solar axion interpretation is, however, in stark contrast with the constraints from stellar astrophysics [163–165].

90.4.3 Conversion of astrophysical axion fluxes

Large-scale B fields exist in astrophysics that can induce axion-photon oscillations. In practical cases, B is much smaller than in the laboratory, whereas the conversion region L is much larger. Therefore, while the product BL can be large, realistic sensitivities are usually restricted to very low-mass particles, far away from the “axion band” in a plot like Fig. 90.2.

One example is SN 1987A, which would have emitted a burst of ALPs due to the Primakoff production in its core. They would have partially converted into γ -rays in the Galactic B -field. The lack of a gamma-ray signal in the GRS instrument of the SMM satellite in coincidence with the observation of the neutrinos emitted from SN 1987A therefore provides a strong bound on their coupling to photons [166, 167]. This bound has been revisited and the underlying physics has been brought to the current state-of-the-art, as far as modeling of the supernova and the Milky-Way magnetic field are concerned, resulting in the limit [168]

$$|g_{a\gamma\gamma}| < 5.3 \times 10^{-12} \text{ GeV}^{-1}, \text{ for } m_a \lesssim 4.4 \times 10^{-10} \text{ eV}, \quad (90.27)$$

see Fig. 90.2.

Reference [169] reports no evidence of a γ -ray burst in observations of extragalactic SNe with the Fermi Large Area Telescope (LAT). Under the assumption that at least one SN was contained within the LAT field of view, the authors derive an upper bound on the axion photon coupling which is about a factor of 5 weaker than the one from SN 1987A, see Fig. 90.2.

The cumulative emission of ALPs from all past core-collapse SNe would lead to a diffuse gamma-ray flux peaked at energies $\sim 50 - 100$ MeV which can convert in the Galactic magnetic field into photons. Using Fermi-LAT measurements of the diffuse γ -ray flux, Ref. [170] obtains a conservative bound on the photon coupling, $|g_{a\gamma\gamma}| < 5 \times 10^{-10} \text{ GeV}^{-1}$, for $m_a \lesssim 10^{-11} \text{ eV}$, see Fig. 90.2, which can be decreased by nearly three orders of magnitude, if an ALP-nucleon coupling of maximal phenomenologically allowed strength, $|g_{aNN}| \sim 10^{-9}$, is allowed.

We use the first observation of Betelgeuse in hard x rays to perform a novel search for axionlike particles (ALPs). Betelgeuse is not expected to be a standard source of x rays, but light ALPs produced in the stellar core could be converted back into photons in the Galactic magnetic field, producing a detectable flux that peaks in the hard x-ray band ($E_\gamma > 10 \text{ keV}$). Using a 50 ks observation of Betelgeuse by the NuSTAR satellite telescope, we find no significant excess of events above the expected background. Using models of the regular Galactic magnetic field in the direction of Betelgeuse, we set a 95% C.L. upper limit on the ALP-photon coupling of $g_{a\gamma} < (0.5 - 1.8) \times 10^{-11} \text{ GeV}^{-1}$ (depending on magnetic field model) for ALP masses $m_a < (5.5 - 3.5) \times 10^{-11} \text{ eV}$.

Hot, young stars, such as Wolf-Rayet stars, are efficiently producing ALPs with energies $\sim 10 - 100$ keV via the Primakoff effect. Large numbers of those stars are hosted by the Galactic Quintuplet and Westerlund 1 super star clusters (SSCs). The non-observation of hard x-rays originating from axion-photon conversion in the Galactic magnetic field in archival NuSTAR (Nuclear Spectroscopic Telescope Array) data from these SSCs allows to set a bound on the axion-photon coupling [171], $|g_{a\gamma\gamma}| < 3.6 \times 10^{-12} \text{ GeV}^{-1}$, for $m_a \lesssim 5 \times 10^{-11} \text{ eV}$, see Fig. 90.2. A somewhat weaker bound in the same mass range was established exploiting NuSTAR data on Betelgeuse [172].

A hard x-ray excess in data from the nearby Magnificent Seven isolated NSs [173] may be explained by ALPs produced in the core those stars and converted in the surrounding magnetic field, with $|g_{aNN}g_{a\gamma\gamma}| \in (2 \times 10^{-21}, 10^{-18}) \text{ GeV}^{-1}$, for $m_a \lesssim 10^{-5} \text{ eV}$ [174]. The non-observation of an x-ray excess from the magnetic white dwarf RE J0317-853 [175] by Chandra yields the constraint $|g_{aee}g_{a\gamma\gamma}| \lesssim 1.3 \times 10^{-25} \text{ GeV}^{-1}$, for $m_a \ll 10^{-5} \text{ eV}$ [176], which provides a non-trivial constraint on the ratio g_{aee}/g_{aNN} for axion models explaining the Magnificent Seven x-ray excess.

90.4.4 Conversion of astrophysical photon fluxes

Magnetically induced oscillations between photons and ALPs can modify the photon fluxes from distant sources in various ways, featuring (i) frequency-dependent dimming, (ii) modified polarization, and (iii) avoiding absorption by propagation in the form of axions.

For example, dimming of SNe Ia could influence the interpretation in terms of cosmic acceleration [177], although it has become clear that photon-ALP conversion could only be a subdominant effect [178]. Searches for linearly polarized emission from magnetized white dwarfs [179] and changes of the linear polarization from radio galaxies (see, e.g., Ref. [180]) provide limits close to $g_{a\gamma\gamma} \sim 10^{-11} \text{ GeV}^{-1}$, for masses $m_a \lesssim 10^{-7} \text{ eV}$ and $m_a \lesssim 10^{-15} \text{ eV}$, respectively, albeit with uncertainties related to the underlying assumptions. Even stronger limits, $g_{a\gamma\gamma} \lesssim 2 \times 10^{-13} \text{ GeV}^{-1}$, for $m_a \lesssim 10^{-14} \text{ eV}$, have been obtained by exploiting high-precision measurements of quasar polarizations [181].

Remarkably, it appears that the Universe could be too transparent to TeV γ -rays that should be absorbed by pair production on the extra-galactic background light [182–186]. The situation is not conclusive at present [187–190], but the possible role of photon-ALP oscillations in TeV γ -ray astronomy is tantalizing [191–193]. Fortunately, the region in ALP parameter space, $g_{a\gamma\gamma} \sim$

$10^{-12} - 10^{-10}$ GeV $^{-1}$ for $m_a \lesssim 10^{-7}$ eV [194], required to explain the anomalous TeV transparency of the Universe, could be conceivably probed by the next generation of laboratory experiments (ALPS II) and helioscopes (IAXO) mentioned above.

This parameter region can also be probed by searching for an irregular behavior of the gamma ray spectrum of distant active galactic nuclei (AGN), expected to arise from photon-ALP mixing in a limited energy range. In this type of studies, the uncertainty in the magnetic field around the source needs to be taken into account. This typically leads to a range of limits on the ALP-photon coupling that depend on the modeling assumptions. The H.E.S.S. collaboration has set a limit of $|g_{a\gamma\gamma}| \lesssim 2.1 \times 10^{-11}$ GeV $^{-1}$, for 1.5×10^{-8} eV $\lesssim m_a \lesssim 6.0 \times 10^{-8}$ eV, from the non-observation of an irregular behavior of the spectrum of the AGN PKS 2155-304 [195], see Fig. 90.2. The Fermi-LAT collaboration has put an even more stringent limit on the ALP-photon coupling [196] from observations of the gamma ray spectrum of NGC 1275, the central galaxy of the Perseus cluster, see Fig. 90.2. A similar analysis has been carried out in Ref. [197], using Fermi-LAT data of PKS 2155-304, and in Ref. [198], using ARGO-YBJ and Fermi-LAT data of Mrk 421 [198], see Fig. 90.2. However, these constraints were obtained under certain theoretical assumptions about magnetic fields surrounding the sources, not confirmed yet by direct astronomical observations in these particular directions; this introduces large systematic uncertainties in the reported constraints [199].

Evidence for spectral irregularities has been reported in Galactic sources, such as pulsars and supernova remnants, and has been interpreted as hints for ALPs [200, 201] (see also discussion in Ref. [202] and references therein). However, the inferred ALP parameters, $|g_{a\gamma\gamma}| \sim 10^{-10}$ GeV $^{-1}$, $m_a \sim$ neV, are in tension with the CAST helioscope bounds. Reference [202] updated the analysis of the pulsar signal region including astrophysical nuisance parameters and correctly deriving confidence intervals on ALP parameters by means of Monte Carlo simulations. The tension with the CAST bounds can be evaded if environmental effects in matter, which would suppress the ALP production in dense astrophysical plasmas like the solar interior, are invoked. If this explanation is correct, the claimed ALP signal would be in reach of the next-generation LSW experiment ALPS II. Other ways to make the CAST bound compatible with photon-ALP conversions in the low-density Galactic medium are invoking photon-ALP-dark photon oscillations [203] or the existence of a number of ‘hidden’ ALPs [204].

At smaller masses, $m_a \lesssim 10^{-12}$ eV, galaxy clusters become highly efficient at interconverting ALPs and photons at x-ray energies. Constraints on spectral irregularities in the spectra of luminous x-ray sources (Hydra A, M87, NGC 1275, NGC 3862, Seyfert galaxy 2E3140; taken by Chandra and XMM-Newton) located in or behind galaxy clusters then lead to stringent upper limits on the ALP-photon coupling [205–210], (for the limits exploiting spectra from Hydra and M87 from Refs. [205] and [207], respectively, see Fig. 90.2). Reference [210] recently performed the most sensitive x-ray searches for ALPs to date by employing Chandra’s High-Energy Transmission Gratings that allow for an unsurpassed spectral resolution. New observations of the AGN NGC 1275 then led to the bound

$$|g_{a\gamma\gamma}| < 8 \times 10^{-13} \text{ GeV}^{-1} \quad (99.7\% \text{ CL}) \quad (90.28)$$

for light ALPs, see Fig. 90.2.

90.4.5 Finite density effects

If the QCD axion sector has a discrete, \mathbb{Z}_N , shift symmetry, its potential is much shallower, and its mass, in units of its decay constant, $m_a f_a \simeq (3\pi)^{-1/4} N^{3/4} 2^{-N/2} m_\pi f_\pi$, is smaller than the one of the canonical QCD axion by an exponential factor $\propto 2^{-N/2}$ [44, 45]. This opens up the parameter space over which one should search for a QCD axion towards the left of the yellow canonical QCD axion band in Fig. 90.1, Fig. 90.2, Fig. 90.3, and Fig. 90.4. Novel bounds apply to this exceptionally light QCD axion due to finite density effects [211–213]. In fact, in dense stellar media, the minimum

of the axion potential may be shifted to π . This has a number of phenomenological consequences that span from the modification of nuclear processes in stars due to $\theta = \mathcal{O}(\pi)$ to modifications in the orbital decay of binary systems (and subsequently in the emitted gravitational waves).

In fact, $\theta \sim 1$ in the solar core would lead to an increased proton-neutron mass difference, which would prohibit the neutrino line corresponding to the ${}^7\text{Be}-{}^7\text{Li}$ mass difference observed by Borexino [214].

Moreover, the fact that the position of the minimum of the axion potential depends on the nuclear density of the medium may also source a long-range force between dense stars [211]. This new long-range force sourced by the axion can be constrained by the measurement of the orbital decay of double pulsar or NS-pulsar binaries [211], Fig. 90.5. The gravitational wave signal of NS-NS mergers or black hole (BH) - NS mergers would also be modified by these axionic long-range forces [211, 212]. A corresponding bound [213] exploiting the gravitational waves observation from the binary NS inspiral GW170817 detected by LIGO (Laser Interferometer Gravitational-Wave Observatory) and Virgo [215] is also plotted in Fig. 90.5.

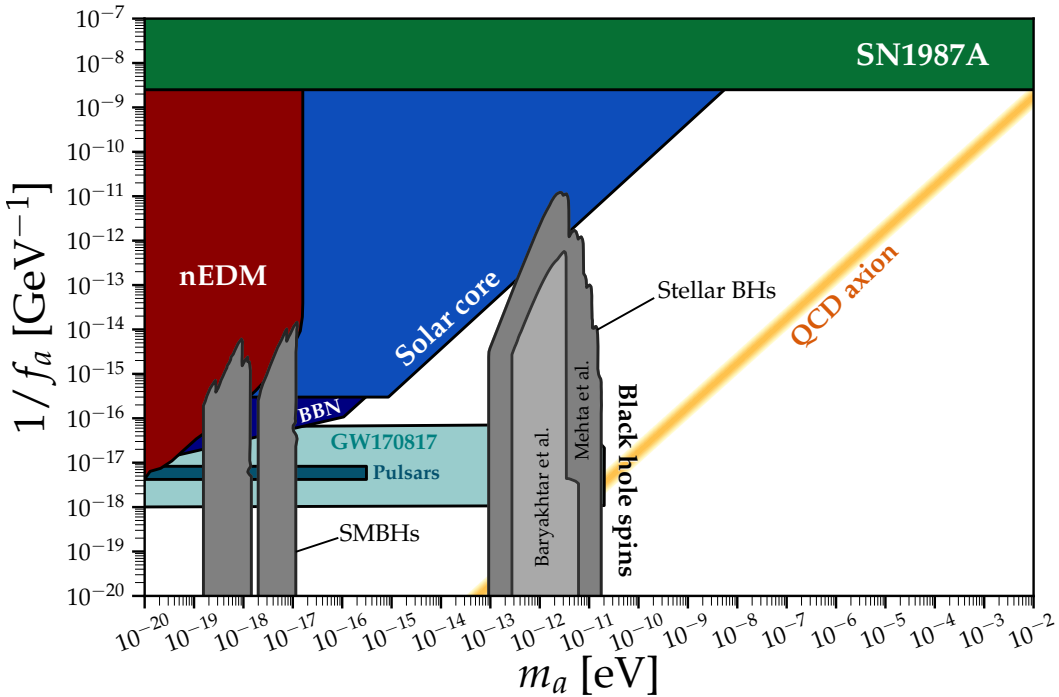


Figure 90.5: Exclusion plot for the QCD axion decay constant as described in the text. Figure courtesy of Ciaran O'Hare [31].

90.4.6 Superradiance of black holes

Light bosonic fields such as axions or ALPs can affect the dynamics and gravitational wave emission of rapidly rotating astrophysical BHs through the superradiance mechanism. When their Compton wavelength is of order of the size of the BH's ergoregion, they form gravitational bound states around the BH. Their occupation number grows exponentially by extracting energy and angular momentum from the black hole, forming a coherent axion or ALP bound state emitting gravitational waves. When accretion cannot replenish the spin of the BH, superradiance dominates the BH spin evolution; this is true for both supermassive and stellar mass BHs. The existence of destabilizing light bosonic fields thus leads to exclusion regions in the mass versus spin plot of

rotating BHs. Stellar BH spin measurements exploiting well-studied binaries and two independent techniques exclude a mass range $6 \times 10^{-13} \text{ eV} < m_a < 2 \times 10^{-11} \text{ eV}$ at 2σ , which for the axion excludes $3 \times 10^{17} \text{ GeV} < f_a < 1 \times 10^{19} \text{ GeV}$ [12, 216, 217]. These bounds apply when gravitational interactions dominate over the axion self-interaction, which is true for the QCD axion in this mass range. Mehta *et al.* [218, 219] considered superradiance bounds for string theory ALPs with a quartic self-coupling (of either sign) given by $\lambda = m_a^2/f_a^2$, using the bosenova model of Ref. [217]. The analysis can be recast into 95% confidence excluded regions in the plane (m_a, f_a) for ALPs, and are shown in Fig. 90.5 (also compiled in Ref. [45]). These bounds were further extended to massive vector and tensor fields in Ref. [220]. Baryakhtar *et al.* [221] used a more advanced model for the effect of self-interactions on superradiant evolution, and a different (frequentist) statistical methodology, leading to more conservative bounds from stellar mass BHs (region near 10^{-12} eV), see Fig. 90.5. Baryakhtar *et al.* [221] vetoed supermassive BHs (SMBHs) with spins measured at low significance, and thus show no bounds in the SMBH region (near 10^{-18} eV); Mehta *et al.* [218–220] included SMBHs in a (quasi-)Bayesian analysis with a flat prior on the spin.

Long lasting, monochromatic gravitational wave signals, which can be distinguished from ordinary astrophysical sources by their clustering in a narrow frequency range, are expected to be produced by axions or ALPs annihilating to gravitons. Gravitational waves could also be sourced by axions/ALPs transitioning between gravitationally bound levels. Accordingly, the gravitational wave detector Advanced LIGO should be sensitive to the axion in the $m_a \lesssim 10^{-10} \text{ eV}$ region. LIGO measurements of BH spins in binary merger events could also provide statistical evidence for the presence of an axion [222, 223]. Similar signatures could arise for supermassive and intermediate mass BHs for particles with masses $\lesssim 10^{-15} \text{ eV}$. Gravitational waves from such sources could be detected at lower-frequency observatories such as LISA (Laser Interferometer Space Antenna).

90.5 Cosmic Axions

90.5.1 Cosmic axion populations

There are two distinct populations of cosmic relic axion populations: a non-thermal one behaving as CDM, and a thermal one comprising a HDM component, in analogy to massive neutrinos. For $m_a \lesssim 0.01 \text{ eV}$, thermal axions are dominantly produced by processes involving quarks and gluons [224, 225], while, for larger masses, the dominant thermalization process is $\pi + \pi \leftrightarrow \pi + a$ [51, 226, 227]. A number of evaluations exploiting cosmological precision data have found restrictive constraints on a possible HDM fraction that translate into an upper bound on the axion mass, $m_a \lesssim 1 \text{ eV}$, if a LO axion-pion chiral effective field theory (EFT) analysis of the axion-pion thermalization rate is used [228–231]. Recently, it was found that the NLO contribution exceeds the LO contributions for masses below $m_a \lesssim 1.2(0.12/C_{a\pi}) \text{ eV}$ [232]. Therefore, in order to assess the reach in sensitivity of future cosmological data sets, one has to improve the EFT description or to compute axion-pion scattering via lattice QCD techniques.

For $m_a \gtrsim 20 \text{ eV}$, axions decay fast on a cosmic time scale, see Eq. (90.8), removing the axion population while injecting photons. This excess radiation provides additional limits on the axion- or ALP-photon coupling up to very large masses masses [233, 234]. In fact, photons from ALP decays could show up as peaks above known backgrounds in galactic x-ray spectra, could contribute to the extragalactic background light (EBL), could ionize primordial hydrogen and thus contribute to the optical depth after recombination, could spoil the agreement of big bang nucleosynthesis (BBN) with observations. The corresponding up-to-date bounds from Refs. [235, 236] are displayed in Fig. 90.2.

The main cosmological interest in axions derives from their possible role as CDM. In addition to thermal processes, axions are abundantly produced by the misalignment (MIS) mechanism [237–239].

The axion DM abundance crucially depends on the cosmological history. Let us first consider the so called *pre-inflationary PQ symmetry breaking scenario*, in which the PQ symmetry is broken before and during inflation and not restored afterwards. After the breakdown of the PQ symmetry, the axion field relaxes somewhere in the bottom of the “wine-bottle-bottom” potential. Near the QCD epoch, topological fluctuations of the gluon fields such as instantons explicitly break the PQ symmetry. This tilting of the “wine-bottle-bottom” drives the axion field toward the *CP*-conserving minimum, thereby exciting coherent oscillations of the axion field that ultimately represent a condensate of CDM. The fractional cosmic mass density in this homogeneous field mode, created by the MIS mechanism, is [30, 240–242],

$$\begin{aligned}\Omega_a^{\text{MIS}} h^2 &\approx 0.12 \left(\frac{f_a}{9 \times 10^{11} \text{ GeV}} \right)^{1.165} F \Theta_i^2 \\ &\approx 0.12 \left(\frac{6 \mu\text{eV}}{m_a} \right)^{1.165} F \Theta_i^2,\end{aligned}\tag{90.29}$$

where h is the present-day Hubble expansion parameter in units of $100 \text{ km s}^{-1} \text{ Mpc}^{-1}$, and $-\pi \leq \Theta_i \leq \pi$ is the initial “misalignment angle” relative to the *CP*-conserving position attained in the causally connected region which evolved into today’s observable Universe. $F = F(\Theta_i, f_a)$ is a factor accounting for anharmonicities in the axion potential. For $F\Theta_i^2 = \mathcal{O}(1)$, m_a should be above $\sim 6 \mu\text{eV}$ in order that the cosmic axion density does not exceed the observed CDM density, $\Omega_{\text{CDM}} h^2 = 0.12$. However, much smaller axion masses (much higher PQ scales) are still possible if entropy is diluted for example by the late decay of a scalar condensate (see for example [243] and references therein) or the initial value Θ_i just happens to be small enough in today’s observable Universe (“anthropic axion window” [244]). In the latter cosmological scenario, however, quantum fluctuations of the axion field during inflation are expected to lead to isocurvature density fluctuations which get imprinted to the temperature fluctuations of the CMB [245, 246]. Their non-observation puts severe constraints on the Hubble expansion rate H_I during inflation [247–251], which read, in the simplest cosmological inflationary scenario,

$$H_I \lesssim 5.7 \times 10^8 \text{ GeV} \left(\frac{5 \text{ neV}}{m_a} \right)^{0.4175},\tag{90.30}$$

if axions represent all of DM. In Ref. [252] an alternative to the MIS mechanism was proposed: the so-called kinetic MIS mechanism. In this case, the axion field is assumed to have an initial velocity which may be generated e.g. by a hypothesized explicit breaking of the axion shift symmetry in the early universe. The amount of QCD axion dark matter generated by the kinetic MIS mechanism can fit the observed dark matter abundance for any $f_a \lesssim 1.5 \times 10^{11} \text{ GeV}$, down to the minimum value allowed by the SN 1987A constraint.

In the *post-inflationary PQ symmetry breaking scenario*, on the other hand, Θ_i will take on different values in different patches of the present Universe. The average contribution is [30, 240–242]

$$\Omega_a^{\text{MIS}} h^2 \approx 0.12 \left(\frac{30 \mu\text{eV}}{m_a} \right)^{1.165}.\tag{90.31}$$

The decay of cosmic strings and domain walls gives rise to a further population of CDM axions, whose abundance suffers from significant uncertainties [241, 242, 253–265] which arise from the difficulty in understanding the energy loss process of topological defects and the generated axion spectrum in a quantitative way. In fact, in the present state-of-the-art it is still possible that the CDM contribution from the decay of topological defects is subdominant [258] or overwhelmingly

large [262] in comparison to the one from the MIS mechanism. Correspondingly, the plausible range of axion masses providing all of CDM in scenarios with postinflationary PQ symmetry breaking is still rather large, namely [258, 262]

$$m_a \approx 26 \text{ } \mu\text{eV} - 0.5 \text{ meV}, \quad (90.32)$$

for models with short-lived (requiring unit color anomaly $N = 1$) domain walls, such as the KSVZ model. For models with long-lived ($N > 1$) domain walls, such as an accidental DFSZ model [266], where the PQ symmetry is broken by higher dimensional Planck suppressed operators, the mass is predicted to be significantly higher [151, 257, 266, 267],

$$m_a \approx (0.58 - 130) \text{ meV}. \quad (90.33)$$

However, the upper part of the predicted range is in conflict with stellar energy-loss limits on the axion.

In this post-inflationary PQ symmetry breakdown scenario, the spatial axion density variations are large at the QCD transition, and they are not erased by free streaming. Gravitationally bound “axion miniclusters” form before and around matter-radiation equality [268–270]. A significant fraction of CDM axions can reside in these bound objects [260, 271]. Remarkably, the minicluster fraction can be bounded by gravitational lensing [272–274], although more simulations are required to understand whether miniclusters are dense enough and survive in sufficient quantities for lensing bounds to apply.

In the above predictions of the fractional cosmic mass density in axions, the exponent, 1.165, arises from the non-trivial temperature dependence of the topological susceptibility $\chi(T) = m_A^2(T)f_A^2$ at temperatures slightly above the QCD quark-hadron phase transition. Lattice QCD calculations of this exponent [30, 275–279], but also Ref. [280], found it to be remarkably close to the prediction of the dilute instanton gas approximation [281] which was previously exploited. Therefore, the state-of-the-art prediction of the axion mass relevant for DM for a fixed initial misalignment angle Θ_i differs from the previous prediction by just a factor of order one.

The non-thermal production mechanisms attributed to axions are generic to light bosonic weakly interacting particles such as ALPs [17]. The relic abundance is set by the epoch when the axion mass becomes significant, $3H(t) \approx m_a(t)$, and ALP field oscillations begin. For ALPs to contribute to the DM density this epoch must precede that of matter radiation equality. For a temperature independent ALP mass this leads to the bound:

$$m_a \gtrsim 7 \times 10^{-28} \text{ eV} \left(\frac{\Omega_m h^2}{0.15} \right)^{1/2} \left(\frac{1 + z_{\text{eq}}}{3.4 \times 10^3} \right)^{3/2}. \quad (90.34)$$

ALPs lighter than this bound are allowed if their cosmic energy density is small, but they are quite distinct from other forms of DM [282]. Ignoring anharmonicities in the ALP potential, and taking the ALP mass to be temperature independent, the relic density in DM ALPs due to the MIS mechanism is given by

$$\Omega_{\text{ALP}}^{\text{MIS}} h^2 = 0.12 \left(\frac{m_a}{4.7 \times 10^{-19} \text{ eV}} \right)^{1/2} \left(\frac{f_a}{10^{16} \text{ GeV}} \right)^2 \left(\frac{\Omega_m h^2}{0.15} \right)^{3/4} \left(\frac{1 + z_{\text{eq}}}{3.4 \times 10^3} \right)^{-3/4} \Theta_i^2. \quad (90.35)$$

An ALP decay constant near the GUT scale gives the correct relic abundance for *ultralight ALPs* (ULAs) with $m_{\text{ULA}} \approx 10^{-19}$ eV [283, 284]. ULAs encompass the entire Earth in a single Compton wavelength, and for large occupation numbers are modelled as a coherent classical field. The

coherence time is determined by the mass and virial velocity in the Milky Way, $\tau_{\text{coh}} \sim 1/m_{\text{ULA}} v_{\text{vir}}^2$, with the detailed properties described by a stochastic model with an approximately Rayleigh Jeans distribution [285]. Natural models for ULAs can be found in string and M-theory compactifications [8–15], in field theory with accidental symmetries [286, 287], or new hidden strongly coupled sectors [288, 289].

In addition to the gravitational potential energy, the ULA field also carries gradient energy. On scales where the gradient energy is non-negligible, ULAs acquire an effective pressure and do not behave as CDM. The gradient energy opposes gravitational collapse, leading to a Jeans scale below which perturbations are stable [290]. The Jeans scale suppresses linear cosmological structure formation relative to CDM [291–293]. The Jeans scale at matter-radiation equality in the case that ULAs make up all of CDM is:

$$k_{J,\text{eq}} = 8.7 \text{ Mpc}^{-1} \left(\frac{1 + z_{\text{eq}}}{3.4 \times 10^3} \right)^{-1/4} \left(\frac{h^2 \Omega_{\text{ALP}}^{\text{MIS}}}{0.12} \right)^{1/4} \left(\frac{m_{\text{ULA}}}{10^{-22} \text{ eV}} \right)^{1/2}. \quad (90.36)$$

On non-linear scales the gradient energy leads to the existence of a class of pseudo-solitons known as oscillatons, or axion stars [294]. Axion stars are expected to form in all cosmological scenarios, and for all types of ALPs, including the QCD axion [295–297].

Cosmological and astrophysical observations are consistent with the CDM model, and departures from it are only allowed on the scales of the smallest observed DM structures with $M \sim 10^{6–8} M_{\odot}$. The CMB power spectrum and galaxy auto-correlation power spectrum limit the ULA mass to $m_{\text{ULA}} \gtrsim \mathcal{O}(\text{few}) \times 10^{-24} \text{ eV}$ from linear theory of structure formation [282, 298]. Analytic models [299] and N -body simulations [300] for non-linear structures show that halo formation is suppressed in ULA models relative to CDM. This leads to constraints on the ULA mass of $m_{\text{ULA}} > 10^{-22} \text{ eV}$ from observations of high- z galaxies [300–302], and $m_{\text{ULA}} > 2 \times 10^{-20} \text{ eV}$ from the Lyman-alpha forest flux power spectrum [303]. Including the effects of anharmonicities on structure formation with ALPs can weaken these bounds if the misalignment angle $\Theta_i \approx \pi$ [304]. A comprehensive study of Milky Way satellites by the DES collaboration resulted in the bound $m_{\text{ULA}} > 2.9 \times 10^{-21} \text{ eV}$ [305]. Cosmological simulations that treat gradient energy in the ULA field beyond the N -body approximation have just recently become available [295, 306–308], and show, among other things, evidence for the formation of axion stars in the centres of ULA halos (various consequences of axion stars are considered in Refs. [309]). These central axion stars have been conjectured to play a role in the apparently cored density profiles of dwarf spheroidal galaxies, and other central galactic regions [295, 310–314]. However, the relationship between the halo mass and the axion star mass [315] leads to problems with this scenario in some galaxies [316–318]. It should be emphasised that many of the conclusions about the role of ULA axion stars in galactic dynamics are based on use of simulation results that do not contain baryons and feedback could be important [319–321].

Inside DM halos the axion gradient energy causes coherence on the de Broglie wavelength and fluctuations on the coherence time [295, 322]. These fluctuations can be thought of as short-lived quasiparticles and lead to relaxation processes that can be described statistically [284, 323] (this relaxation processes also leads to the gravitational condensation of axion stars [296]). The typical relaxation time is:

$$t \sim 10^{10} \text{ years} \left(\frac{m_{\text{ULA}}}{10^{-22} \text{ eV}} \right)^3 \left(\frac{v}{100 \text{ km s}^{-1}} \right)^2 \left(\frac{r}{5 \text{ kpc}} \right)^4, \quad (90.37)$$

where v and r are the velocity and radius of the orbit in the host DM halo.

Relaxation processes such as these are not observed in galaxies, though there are some circumstances where they may be desirable [284]. An absence of observed relaxation can be used

to set limits on the ULA mass. An absence of Milky Way disk thickening excludes $m_{\text{ULA}} > 0.6 \times 10^{-22} \text{ eV}$ [324], while stellar streams give the stronger bound $m_{\text{ULA}} > 1.5 \times 10^{-22} \text{ eV}$ [325]. The survival of the old star cluster in Eridanus II [326] excludes the range of masses $10^{-21} \text{ eV} \lesssim m_{\text{ULA}} \lesssim 10^{-19} \text{ eV}$ [327]. As in the case of ULA axion stars, current constraints from heating do not fully account for the possible role of baryons.

Finally, one should note that the beyond-CDM physics of ULAs (Jeans scale, relaxation, axion star formation) of course also applies to the QCD axion on smaller length scales. This is of particular interest inside axion miniclusters [268, 269, 296, 297].

90.5.2 Electron recoil searches

In a DM direct detection experiment, a DM ALP featuring a coupling to the electron can be absorbed by the target material, leading to a mono-energetic electronic recoil signal peaked at m_a . This mechanism allowed the EDELWEISS [328], PandaX [329], SuperCDMS [330] and XENON1T [331] collaborations to put the bounds on the axion-electron coupling displayed in Fig. 90.3 in the keV mass range.

90.5.3 Telescope searches

The two-photon decay is extremely slow for axions with masses in the CDM regime, but could be detectable for eV masses. The signature would be a quasi-monochromatic emission line from galaxies and galaxy clusters. The expected optical line intensity for DFSZ axions is similar to the continuum night emission. A search for optical line emission in two Abell clusters using spectra from the VIMOS (Visible Multi-Object Spectrograph) integral field unit at the Very Large Telescope (VLT) excludes axions and ALPs with a two photon coupling bigger than $\sim 5 \times 10^{-12} \text{ GeV}^{-1}$ in the mass range between 4.5 and 5.5 eV, see Fig. 90.2. Spectral data on the dwarf spheroidal galaxy Leo T from the Multi Unit Spectroscopic Explorer (MUSE) at the VLT improve these constraints by more than an order of magnitude for ALP masses between 2.7 and 5.3 eV [332], see Fig. 90.2.

Very low-mass axions in halos produce a weak quasi-monochromatic radio line. Virial velocities in undisrupted dwarf galaxies are very low, and the axion decay line would therefore be extremely narrow. A search with the Haystack radio telescope on three nearby dwarf galaxies provided a limit $|g_{a\gamma\gamma}| < 1.0 \times 10^{-9} \text{ GeV}^{-1}$ at 96% CL for $298 < m_a < 363 \mu\text{eV}$ [333]. However, this combination of m_a and $g_{a\gamma\gamma}$ does not exclude plausible axion models.

A monochromatic signal is also produced in the conversion of DM axions in the background of slowly varying galactic B -fields [334]. The signal is, however, sensitive to magnetic field power on the scale of the axion mass [335]. Present and future radio telescopes appear to be able to probe ALP DM in the mass range $0.1 - 100 \mu\text{eV}$ for couplings $g_{a\gamma\gamma} \gtrsim 10^{-13} \text{ GeV}^{-1}$ [335] – unfortunately not reaching down to the benchmark QCD axion sensitivity.

Resonant conversion of QCD axion or ALP DM in NS magnetospheres may give a detectable signal from individual NSs for axion masses in the μeV range [336]. Recent analyses of radio data in the frequency range 1-40 GHz from several NSs have found no evidence for a narrow peak predicted from this mechanism and therefore put bounds on the axion-photon coupling around $10^{-11} \text{ GeV}^{-2}$ for $4 \lesssim m_a \lesssim 160 \text{ GHz}$ [337–339], see Fig. 90.2. However, these limits may still suffer from significant uncertainties because the line intensity is difficult to predict in detail in the complicated environments of NSs [339–342]. Stimulated ALP decays in high radiation environments may be detectable, by next-generation radio telescopes such as the Square Kilometer Array, down to $g_{a\gamma\gamma} \gtrsim 10^{-11} \text{ GeV}^{-1}$, for masses between μeV and 0.1 meV [343]. Furthermore, in condensed ALP dark matter structures such as ALP stars, a parametric instability may lead to an exponential enhancement of the photon flux from ALP-photon conversion by a factor $\sim \exp \left[|g_{a\gamma\gamma}| \int ds \rho_a^{1/2}(s) \right]$, where the integral is along any photon trajectory through the ALP overdensity [344, 345].

Photon propagation on an ULA DM background can induce birefringence that can be compared

with upper limits from the CMB [346–348] and may also be probed with other sources such as pulsars [349].

90.5.4 Microwave cavity experiments

Over a large part of the plausible m_a range for CDM, Galactic halo axions may be detected by their resonant conversion into a quasi-monochromatic microwave signal in a high-Q electromagnetic cavity permeated by a strong, static B field [7, 350, 351]. The cavity frequency is tunable, and the signal is maximized when the resonant frequency is the total axion energy, rest mass plus kinetic energy, of $\nu = (m_a/2\pi)[1 + \mathcal{O}(10^{-6})]$, the width above the rest mass representing the axions' virial distribution in the galaxy near Earth. The frequency spectrum may also contain finer structure from axions more recently fallen into the galactic potential and not yet completely virialized [352, 353] or otherwise incompletely thermalized.

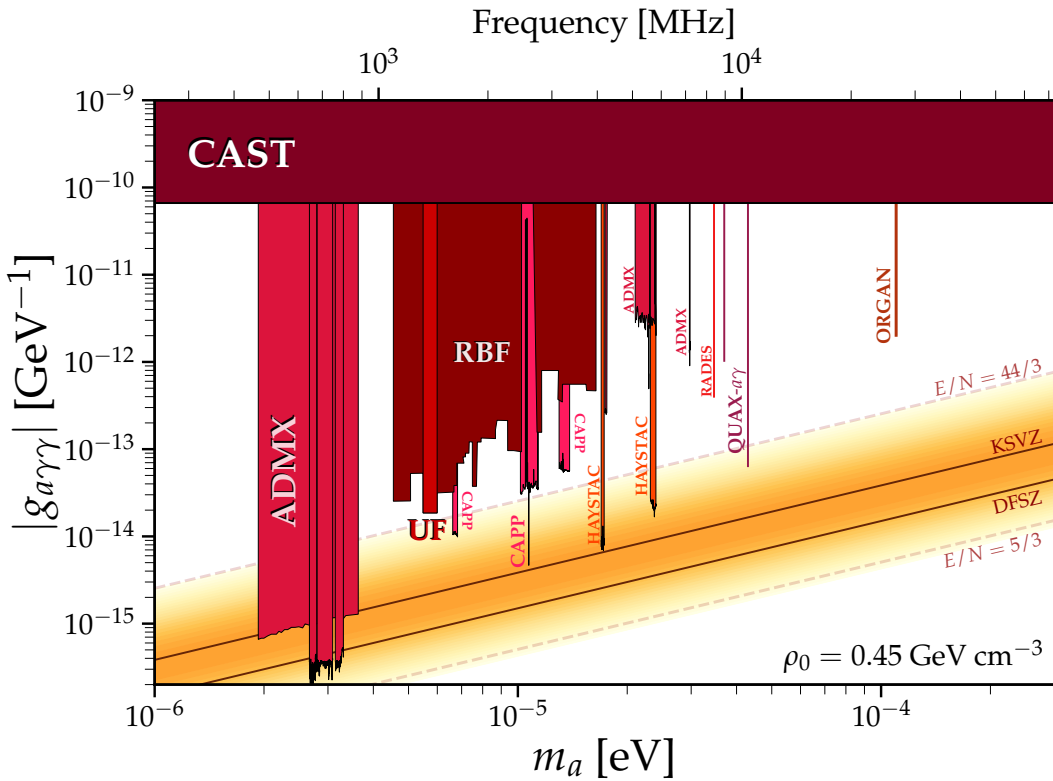


Figure 90.6: Exclusion plot for ALP-photon coupling with closeup on the parameter space of RF cavity experiments as described in the text. Figure courtesy of Ciaran O'Hare [31].

The feasibility of this technique was established in early experiments (RBF (Rochester-Brookhaven-Florida) and UF (University of Florida)) of relatively small sensitive volume, $\mathcal{O}(1 \text{ liter})$, with HFET-based microwave amplifiers, setting limits in the range $4.5 < m_a < 16.3 \mu\text{eV}$ [354–356], but lacking by 2–3 orders of magnitude the sensitivity required to detect realistic axions, see Fig. 90.6.

Later, the first generation of ADMX ($B \sim 8 \text{ T}$, $V \sim 200 \text{ liters}$) achieved sensitivity to KSVZ axions, assuming they saturate the local DM density and are well virialized, over the mass range 1.9 – $3.3 \mu\text{eV}$ [357]. Should halo axions have a significant narrow component not yet virialized, ADMX was sensitive to DFSZ axions over the entire mass range [358]. The corresponding 90% CL exclusion regions shown in Fig. 90.6 assume a local CDM density of $7.5 \times 10^{-25} \text{ g cm}^{-3}$ (450 MeV cm^{-3}).

Somewhat later, the ADMX experiment commissioned an upgrade [359] that replaced the microwave HFET amplifiers by near-quantum-limited low-noise dc SQUID microwave amplifiers [360] and, more recently, with Josephson parametric amplifiers (related to the earlier dc SQUID amplifiers), also with noise near-quantum-limited [361]. With its large volume and low noise, ADMX has achieved an unprecedented axion DM sensitivity in the mass range between 2.66 and $3.31\text{ }\mu\text{eV}$ [362–364], down to the DFSZ benchmark axion-photon coupling, see Fig. 90.6. This apparatus is also sensitive to certain other hypothetical light bosons, such as hidden photons or chameleons, over a limited parameter space [17, 365, 366].

ADMX also deployed a testbed experiment to probe higher masses. This experiment – ADMX-Sidecar – sharing the magnet bore and operating in tandem with the main ADMX experiment, searches in three widely spaced frequency ranges (4202–4249 MHz, 5086–5799 MHz and 7173–7203 MHz), using both the TM_{010} and TM_{020} cavity modes, and demonstrating the use of a piezoelectric actuator for cavity tuning in the high-vacuum, high magnetic field, cryogenic environment [367].

The HAYSTAC experiment reported results from a microwave cavity search for DM axions with masses above $20\text{ }\mu\text{eV}$. They exclude axions with two-photon coupling $|g_{a\gamma\gamma}| \gtrsim 2 \times 10^{-14}\text{ GeV}^{-1}$ over the range $23.15\text{ }\mu\text{eV} < m_a < 24.0\text{ }\mu\text{eV}$ [368, 369], a factor of 2.7 above the KSVZ coupling benchmark, see Fig. 90.6. With a Josephson parametric amplifier, this experiment has demonstrated system noise approaching the “standard quantum limit” for the first time in an axion search. More recently, HAYSTAC explored state squeezing to reduce the system noise, where the squeezed quadrature had lower noise relative to that of the “standard quantum limit”, thereby reducing the scan time by a factor of around 2 over a narrow mass range. This resulted in limits on $|g_{a\gamma\gamma}|$ about a factor of 1.4 above the KSVZ benchmark coupling over the axion-mass ranges $16.96\text{ }\mu\text{eV} < m_a < 17.12\text{ }\mu\text{eV}$ and $17.14\text{ }\mu\text{eV} < m_a < 17.28\text{ }\mu\text{eV}$ at 90% CL [370] as shown in Fig. 90.6.

The ORGAN experiment aims to probe axions over the relatively high-mass range $60\text{ }\mu\text{eV} < m_a < 210\text{ }\mu\text{eV}$, which includes axion masses motivated by postinflationary PQ symmetry breaking. ORGAN is based on long, thin cavities with this early generation not being tunable and operating in the TM_{020} mode. In this pathfinding run, it set the limit $|g_{a\gamma\gamma}| < 2 \times 10^{-12}\text{ GeV}^{-1}$ at $110\text{ }\mu\text{eV}$ across a narrow mass range 2.5 neV [371], see Fig. 90.6. Another non-tunable experiment is QUAX a- γ , a haloscope of otherwise conventional design sensitivity a factor of approximately 5 above the benchmark KSVZ coupling at two narrowband ranges near 10 GHz [372, 373], see Fig. 90.6. Other cavity detectors are moving into operation, including an experiment with unusual high-aspect-ratio cavities in the CAST bore (CAST-RADES [374]).

CAPP is an ambitious program to search for axions across a wide mass range at high sensitivity. Recently the CAPP-8TB detector has reported results approaching KSVZ sensitivity in the mass range $6.62\text{--}8.82\text{ }\mu\text{eV}$ [375]. A further refinement is searching the higher frequencies allowed by subdividing a cavity into smaller higher-frequency cells. Such a multi-cell cavity system has reported sensitivity around an order-of-magnitude above the KSVZ benchmark coupling in the mass range $13.0\text{--}13.9\text{ }\mu\text{eV}$ [376], see Fig. 90.6. The CAPP-PACE detector has reported limits around KSVZ benchmark sensitivity in the mass range $10.7126\text{--}10.7186\text{ }\mu\text{eV}$ and around an order-of-magnitude above benchmark KSVZ coupling in the mass range $10.16\text{--}10.37$ [377], see Fig. 90.6.

90.5.5 New concepts for axion DM direct detection

Other new concepts for searching for axion DM are also being investigated. An alternative to the microwave cavity technique is based on a novel detector architecture consisting of an open, Fabry-Perot resonator and a series of current-carrying wire planes [378]. The Orpheus detector has demonstrated this new technique, excluding DM ALPs with masses between 68.2 and $76.5\text{ }\mu\text{eV}$ and axion-photon couplings greater than $4 \times 10^{-7}\text{ GeV}^{-1}$. This technique may be able to probe DM axions in the mass range from 40 to $700\text{ }\mu\text{eV}$. “Plasma haloscopes” are under development by

the ALPHA collaboration [379]. This concept uses a metamaterial consisting of spaced out wires, inducing an effective photon mass, tunable with wire separation, and sensitive to axion masses 35–400 μeV . Another detector concept exploits the fact that a magnetized mirror would radiate photons in the background of axion DM, which could be collected like in a dish antenna [380]. The proposed MADMAX experiment will place a stack of dielectric layers in a magnetic field in order to resonantly enhance the photon signal, aiming a sensitivity to probe the mass range $40 \mu\text{eV} \lesssim m_a \lesssim 200 \mu\text{eV}$ [381,382]. Optical dielectric haloscopes with single photon signal detection have been proposed to search for axions in the 50 meV – 10 eV mass range [383]. Absorption of axions on molecular transitions can be sensitive to the axion pseudoscalar coupling $g_{aN\gamma}$ to nucleons or the pseudoscalar coupling g_{aee} to electrons in the 0.5 – 20 eV range [384]. It has also been pointed out that the coupling induced by an axion field between photonic modes [385,386] or atomic states [387] separated by an energy equal to the axion mass may be leveraged for axion detection, though the implementation may be challenging. Certain magnetic topological insulators are conjectured to contain axion-polaritons, quasiparticles composed of magnons and the electric field, with magnetically tunable mass in the meV to eV range [388–390]. Axion dark matter leads to resonant photon emission from such materials, which can be detected [391,392].

In the intermediate mass region, $\text{neV} \lesssim m_a \lesssim 0.1 \mu\text{eV}$, one may exploit a cooled LC circuit and precision magnetometry to search for the oscillating electric current induced by DM axions in a strong magnetic field [393,394]. A number of small-scale pathfinder experiments have implemented this approach: ABRACADABRA [395,396] used a nonresonant configuration in a toroidal magnet for a broadband search, ADMX-SLIC [397] used a resonant configuration in a solenoid magnet for a narrowband search, SHAFT [398] used a nonresonant configuration in a toroidal magnet enhanced with a ferromagnetic core, and BASE [399] used antiprotons in a Penning trap as the LC circuit. The exclusion limits from these experiments are shown in Fig. 90.2; none are yet sensitive to the QCD axion. Future work in this direction is expected to have much more competitive limits [400].

The oscillating Galactic DM axion field induces oscillating nuclear electric dipole moments (EDMs) [138],

$$d_N(t) = g_{aN\gamma} \sqrt{2\rho_{a\text{DM}}} \cos(m_a t)/m_a, \quad (90.38)$$

where $g_{aN\gamma}$ is the coupling of the axion to the nucleon EDM operator, defined in Eq. (90.4). An analysis of the ratio of spin-precession frequencies of stored ultracold neutrons and ^{199}Hg atoms measured by neutron EDM experiments for an axion-induced oscillating neutron EDM revealed no signal consistent with axion DM, excluding a sizeable region of parameter space in the mass region $10^{-24} \text{ eV} \leq m_a \leq 10^{-17} \text{ eV}$ [401], which surpass the limits on anomalous energy loss of SN 1987A by more than seven orders of magnitude, see Fig. 90.1, and are competitive with the ones from the requirement of successful BBN established in [402], see Fig. 90.5.¹ In fact, the oscillating dark matter axion field could increase the neutron-proton mass difference at neutron freeze-out and thus result in the underproduction of ^4He during BBN. The oscillating EDMs cause also the precession of nuclear spins in a nucleon spin polarized sample in the presence of an electric field. The resulting transverse magnetization can be searched for by exploiting magnetic-resonance (MR) techniques, which are most sensitive in the range of low oscillation frequencies corresponding to sub-neV axion masses. The aim of the corresponding Cosmic Axion Spin Precession Experiment (CASPER) [403] is to probe axion DM in the anthropic window, $f_a \gtrsim 10^{15} \text{ GeV}$ ($m_a \lesssim \text{neV}$), motivated from Grand Unification [404–407]. There are two interactions probed through MR: the electric dipole coupling as searched for by CASPER-electric, whose first run has established the limits shown in Fig. 90.1 [408], and an interaction between the axion field gradient and the

¹These limits are still to the left of the canonical QCD axion line. However, in non-minimal models where the QCD axion is a mediator between strongly interacting hidden sectors enjoying a discrete, \mathbb{Z}_N , shift symmetry, the QCD axion line can be shifted to the left in discrete steps, without any fine tuning [44,45,289].

nuclear spin, which is aimed for by CASPER-wind. In the meantime, the latter has been explored through comagnetometry between a variety of nuclei: H-¹²C in CASPER-ZULF [409, 410], Xe-Rb in NASDUCK [411], and K-³He [412, 413]. The exclusions from these searches are shown in Fig. 90.4. Sub- μ eV ALP masses can also be probed by using the storage ring EDM method proposed in Ref. [414] which exploits a combination of B and E-fields to produce a resonance between the $g - 2$ spin precession frequency and the DM ALP field oscillation frequency. This method, however, does not reach the sensitivity to probe the QCD axion prediction for $g_{aN\gamma}$. An eventually non-zero axion electron coupling g_{aee} will lead to an electron spin precession about the axion DM wind [415, 416]. The QUAX a-e experiment exploits MR inside a magnetized material [417]. Because of the higher Larmor frequency of the electron, it is sensitive in the classic window. Its first run established the bound in the mass range 42.4 to 43.2 μ eV [418], slightly better than the solar ν bound, shown in Fig. 90.3.

90.6 Conclusions

There is a strengthening physics case for very weakly coupled light particles beyond the Standard Model. The elegant solution of the strong CP problem proposed by Peccei and Quinn yields a particularly strong motivation for the axion. In many theoretically appealing ultraviolet completions of the Standard Model axions and ALPs occur automatically. Moreover, they are natural CDM candidates. Perhaps the first hints of their existence have already been seen in the anomalous excessive cooling of stars and the anomalous transparency of the Universe for very high energy gamma rays. Interestingly, a significant portion of previously unexplored, but phenomenologically very interesting and theoretically very well motivated axion and ALP parameter space can be tackled in the foreseeable future by a number of terrestrial experiments searching for axion/ALP DM, for solar axions/ALPs, and for light apparently shining through a wall.

90.7 Acknowledgements

It is a pleasure to thank Masha Baryakhtar, Francesca Calore, Luca Di Luzio, Andrew Geraci, Maurizio Giannotti, Igor Irastorza, David J.E. Marsh, Alessandro Mirizzi, Benjamin Safdi, Ken'ichi Saikawa, Yannis Semertzidis, Guenter Sigl, and Sergey Troitsky for discussions, suggestions, and comments on this review. Particular thanks to Ciaran O'Hare for maintaining a publicly accessible collection of axion plots and providing updates to accomodate this review [31].

References

- [1] R. D. Peccei and H. R. Quinn, *Phys. Rev. Lett.* **38**, 1440 (1977).
- [2] R. D. Peccei and H. R. Quinn, *Phys. Rev.* **D16**, 1791 (1977).
- [3] S. Weinberg, *Phys. Rev. Lett.* **40**, 223 (1978).
- [4] F. Wilczek, *Phys. Rev. Lett.* **40**, 279 (1978).
- [5] Y. Chikashige, R.N. Mohapatra, and R.D. Peccei, *Phys. Lett.* **B98**, 265 (1981).
- [6] G. B. Gelmini and M. Roncadelli, *Phys. Lett.* **99B**, 411 (1981).
- [7] P. Sikivie, *Phys. Rev. Lett.* **51**, 1415 (1983) and Erratum *ibid.*, **52**, 695 (1984).
- [8] E. Witten, *Phys. Lett.* **149B**, 351 (1984).
- [9] J. P. Conlon, *JHEP* **05**, 078 (2006), [[hep-th/0602233](#)].
- [10] P. Svrcek and E. Witten, *JHEP* **06**, 051 (2006), [[hep-th/0605206](#)].
- [11] K.-S. Choi *et al.*, *Phys. Lett.* **B675**, 381 (2009), [[arXiv:0902.3070](#)].
- [12] A. Arvanitaki *et al.*, *Phys. Rev.* **D81**, 123530 (2010), [[arXiv:0905.4720](#)].
- [13] B. S. Acharya, K. Bobkov and P. Kumar, *JHEP* **11**, 105 (2010), [[arXiv:1004.5138](#)].
- [14] M. Cicoli, M. Goodsell and A. Ringwald, *JHEP* **10**, 146 (2012), [[arXiv:1206.0819](#)].

- [15] J. Halverson, C. Long and P. Nath, *Phys. Rev.* **D96**, 5, 056025 (2017), [[arXiv:1703.07779](#)].
- [16] A. E. Nelson and J. Scholtz, *Phys. Rev. D* **84**, 103501 (2011), [[arXiv:1105.2812](#)].
- [17] P. Arias *et al.*, *JCAP* **1206**, 013 (2012), [[arXiv:1201.5902](#)].
- [18] P. W. Graham, J. Mardon and S. Rajendran, *Phys. Rev. D* **93**, 10, 103520 (2016), [[arXiv:1504.02102](#)].
- [19] J. Jaeckel and A. Ringwald, *Ann. Rev. Nucl. Part. Sci.* **60**, 405 (2010), [[arXiv:1002.0329](#)].
- [20] A. Ringwald, *Phys. Dark Univ.* **1**, 116 (2012), [[arXiv:1210.5081](#)].
- [21] J. Jaeckel, *Frascati Phys. Ser.* **56**, 172 (2012), [[arXiv:1303.1821](#)].
- [22] A. Caputo *et al.* (2021), [[arXiv:2105.04565](#)].
- [23] M. Pospelov and A. Ritz, *Nucl. Phys.* **B573**, 177 (2000), [[hep-ph/9908508](#)].
- [24] C. A. Baker *et al.*, *Phys. Rev. Lett.* **97**, 131801 (2006), [[hep-ex/0602020](#)].
- [25] C. Abel *et al.* (nEDM), *Phys. Rev. Lett.* **124**, 8, 081803 (2020), [[arXiv:2001.11966](#)].
- [26] H. Georgi, D. B. Kaplan and L. Randall, *Phys. Lett.* **169B**, 73 (1986).
- [27] R. J. Crewther, *Phys. Lett.* **70B**, 349 (1977).
- [28] P. Di Vecchia and G. Veneziano, *Nucl. Phys.* **B171**, 253 (1980).
- [29] M. Gorghetto and G. Villadoro, *JHEP* **03**, 033 (2019), [[arXiv:1812.01008](#)].
- [30] S. Borsanyi *et al.*, *Nature* **539**, 7627, 69 (2016), [[arXiv:1606.07494](#)].
- [31] C. O’Hare, “cajohare/axionlimits: Axionlimits,” (2020), URL <https://doi.org/10.5281/zenodo.3932430>.
- [32] J. E. Kim, *Phys. Rev. Lett.* **43**, 103 (1979).
- [33] M. A. Shifman, A. I. Vainshtein and V. I. Zakharov, *Nucl. Phys.* **B166**, 493 (1980).
- [34] M. Dine, W. Fischler and M. Srednicki, *Phys. Lett.* **104B**, 199 (1981).
- [35] A. R. Zhitnitsky, *Sov. J. Nucl. Phys.* **31**, 260 (1980), [*Yad. Fiz.* 31, 497 (1980)].
- [36] J. E. Kim and G. Carosi, *Rev. Mod. Phys.* **82**, 557 (2010), [[arXiv:0807.3125](#)].
- [37] G. Grilli di Cortona *et al.*, *JHEP* **01**, 034 (2016), [[arXiv:1511.02867](#)].
- [38] J. E. Kim, *Phys. Rev. D* **58**, 055006 (1998), [[hep-ph/9802220](#)].
- [39] L. Di Luzio, F. Mescia and E. Nardi, *Phys. Rev. Lett.* **118**, 3, 031801 (2017), [[arXiv:1610.07593](#)].
- [40] L. Di Luzio, F. Mescia and E. Nardi, *Phys. Rev. D* **96**, 7, 075003 (2017), [[arXiv:1705.05370](#)].
- [41] L. Di Luzio *et al.*, *Phys. Rept.* **870**, 1 (2020), [[arXiv:2003.01100](#)].
- [42] M. Farina *et al.*, *JHEP* **01**, 095 (2017), [[arXiv:1611.09855](#)].
- [43] P. Agrawal *et al.*, *JHEP* **02**, 006 (2018), [[arXiv:1709.06085](#)].
- [44] A. Hook, *Phys. Rev. Lett.* **120**, 26, 261802 (2018), [[arXiv:1802.10093](#)].
- [45] L. Di Luzio *et al.*, *JHEP* **05**, 184 (2021), [[arXiv:2102.00012](#)].
- [46] A. V. Sokolov and A. Ringwald, *JHEP* **06**, 123 (2021), [[arXiv:2104.02574](#)].
- [47] G. Raffelt and D. Seckel, *Phys. Rev. Lett.* **60**, 1793 (1988).
- [48] M. Carena and R. D. Peccei, *Phys. Rev. D* **40**, 652 (1989).
- [49] K. Choi, K. Kang and J. E. Kim, *Phys. Rev. Lett.* **62**, 849 (1989).
- [50] M. Srednicki, *Nucl. Phys.* **B260**, 689 (1985).
- [51] S. Chang and K. Choi, *Phys. Lett.* **B316**, 51 (1993), [[hep-ph/9306216](#)].

- [52] C.-Y. Chen and S. Dawson, *Phys. Rev.* **D87**, 055016 (2013), [[arXiv:1301.0309](#)].
- [53] D. A. Dicus *et al.*, *Phys. Rev.* **D18**, 1829 (1978).
- [54] G. Raffelt and L. Stodolsky, *Phys. Rev.* **D37**, 1237 (1988).
- [55] A. A. Anselm, *Yad. Fiz.* **42**, 1480 (1985).
- [56] K. van Bibber *et al.*, *Phys. Rev. Lett.* **59**, 759 (1987).
- [57] G. Ruoso *et al.*, *Z. Phys.* **C56**, 505 (1992).
- [58] R. Cameron *et al.*, *Phys. Rev.* **D47**, 3707 (1993).
- [59] M. Fouche *et al.*, *Phys. Rev.* **D78**, 032013 (2008), [[arXiv:0808.2800](#)].
- [60] P. Pugnat *et al.* (OSQAR), *Phys. Rev.* **D78**, 092003 (2008), [[arXiv:0712.3362](#)].
- [61] A. S. Chou *et al.* (GammeV (T-969)), *Phys. Rev. Lett.* **100**, 080402 (2008), [[arXiv:0710.3783](#)].
- [62] A. Afanasev *et al.*, *Phys. Rev. Lett.* **101**, 120401 (2008), [[arXiv:0806.2631](#)].
- [63] K. Ehret *et al.* (ALPS), *Phys. Lett.* **B689**, 149 (2010), [[arXiv:1004.1313](#)].
- [64] P. Pugnat *et al.* (OSQAR), *Eur. Phys. J.* **C74**, 8, 3027 (2014), [[arXiv:1306.0443](#)].
- [65] R. Ballou *et al.* (OSQAR), *Phys. Rev.* **D92**, 9, 092002 (2015), [[arXiv:1506.08082](#)].
- [66] F. Hoogeveen and T. Ziegenhagen, *Nucl. Phys.* **B358**, 3 (1991).
- [67] P. Sikivie, D. B. Tanner and K. van Bibber, *Phys. Rev. Lett.* **98**, 172002 (2007), [[hep-ph/0701198](#)].
- [68] G. Mueller *et al.*, *Phys. Rev.* **D80**, 072004 (2009), [[arXiv:0907.5387](#)].
- [69] R. Bähre *et al.*, *JINST* **8**, T09001 (2013), [[arXiv:1302.5647](#)].
- [70] F. Hoogeveen, *Phys. Lett.* **B288**, 195 (1992).
- [71] J. Jaeckel and A. Ringwald, *Phys. Lett.* **B659**, 509 (2008), [[arXiv:0707.2063](#)].
- [72] F. Caspers, J. Jaeckel and A. Ringwald, *JINST* **4**, P11013 (2009), [[arXiv:0908.0759](#)].
- [73] R. Povey, J. Hartnett and M. Tobar, *Phys. Rev.* **D82**, 052003 (2010), [[arXiv:1003.0964](#)].
- [74] M. Betz *et al.*, *Phys. Rev.* **D88**, 7, 075014 (2013), [[arXiv:1310.8098](#)].
- [75] L. Maiani, R. Petronzio and E. Zavattini, *Phys. Lett.* **B175**, 359 (1986).
- [76] Y. Semertzidis *et al.*, *Phys. Rev. Lett.* **64**, 2988 (1990).
- [77] E. Zavattini *et al.* (PVLAS), *Phys. Rev. Lett.* **96**, 110406 (2006), [Erratum: *Phys. Rev. Lett.* 99, 129901(2007)], [[hep-ex/0507107](#)].
- [78] E. Zavattini *et al.* (PVLAS), *Phys. Rev.* **D77**, 032006 (2008), [[arXiv:0706.3419](#)].
- [79] F. Della Valle *et al.*, *Eur. Phys. J.* **C76**, 1, 24 (2016), [[arXiv:1510.08052](#)].
- [80] E. Fischbach and C. Talmadge, *Nature* **356**, 207 (1992).
- [81] J. E. Moody and F. Wilczek, *Phys. Rev.* **D30**, 130 (1984).
- [82] A. N. Youdin *et al.*, *Phys. Rev. Lett.* **77**, 2170 (1996).
- [83] W.-T. Ni *et al.*, *Phys. Rev. Lett.* **82**, 2439 (1999).
- [84] D. F. Phillips *et al.*, *Phys. Rev.* **D63**, 111101 (2001), [[arXiv:physics/0008230](#)].
- [85] B. R. Heckel *et al.*, *Phys. Rev. Lett.* **97**, 021603 (2006), [[hep-ph/0606218](#)].
- [86] S. A. Hoedl *et al.*, *Phys. Rev. Lett.* **106**, 041801 (2011).
- [87] E. G. Adelberger *et al.*, *Phys. Rev. Lett.* **98**, 131104 (2007), [[hep-ph/0611223](#)].
- [88] D. J. Kapner *et al.*, *Phys. Rev. Lett.* **98**, 021101 (2007), [[hep-ph/0611184](#)].
- [89] G. Raffelt, *Phys. Rev.* **D86**, 015001 (2012), [[arXiv:1205.1776](#)].

- [90] C. A. J. O'Hare and E. Vitagliano, *Phys. Rev. D* **102**, 11, 115026 (2020), [[arXiv:2010.03889](#)].
- [91] A. Arvanitaki and A. A. Geraci, *Phys. Rev. Lett.* **113**, 16, 161801 (2014), [[arXiv:1403.1290](#)].
- [92] A. A. Geraci *et al.* (ARIADNE), *Springer Proc. Phys.* **211**, 151 (2018), [[arXiv:1710.05413](#)].
- [93] H. Fosbinder-Elkins *et al.* (2017), [[arXiv:1710.08102](#)].
- [94] N. Aggarwal *et al.* (ARIADNE) (2020), [[arXiv:2011.12617](#)].
- [95] M. S. Turner, *Phys. Rept.* **197**, 67 (1990).
- [96] G. G. Raffelt, *Lect. Notes Phys.* **741**, 51 (2008), [,51(2006)], [[hep-ph/0611350](#)].
- [97] S. Andriamonje *et al.* (CAST), *JCAP* **0704**, 010 (2007), [[hep-ex/0702006](#)].
- [98] P. Gondolo and G. G. Raffelt, *Phys. Rev. D* **79**, 107301 (2009), [[arXiv:0807.2926](#)].
- [99] H. Schlattl, A. Weiss and G. Raffelt, *Astropart. Phys.* **10**, 353 (1999), [[hep-ph/9807476](#)].
- [100] N. Vinyoles *et al.*, *JCAP* **1510**, 10, 015 (2015), [[arXiv:1501.01639](#)].
- [101] A. Ayala *et al.*, *Phys. Rev. Lett.* **113**, 19, 191302 (2014), [[arXiv:1406.6053](#)].
- [102] O. Straniero *et al.*, in “Proceedings, 11th Patras Workshop on Axions, WIMPs and WISPs (Axion-WIMP 2015): Zaragoza, Spain, June 22-26, 2015,” 77–81 (2015).
- [103] J. Redondo, *JCAP* **1312**, 008 (2013), [[arXiv:1310.0823](#)].
- [104] O. Straniero *et al.*, *Astron. Astrophys.* **644**, A166 (2020), [[arXiv:2010.03833](#)].
- [105] F. Capozzi and G. Raffelt, *Phys. Rev. D* **102**, 8, 083007 (2020), [[arXiv:2007.03694](#)].
- [106] G. G. Raffelt, *Phys. Lett.* **166B**, 402 (1986).
- [107] S. I. Blinnikov and N. V. Dunina-Barkovskaya, *Mon. Not. Roy. Astron. Soc.* **266**, 289 (1994).
- [108] M. M. Miller Bertolami *et al.*, *JCAP* **1410**, 10, 069 (2014), [[arXiv:1406.7712](#)].
- [109] J. Isern *et al.*, *Astrophys. J.* **682**, L109 (2008), [[arXiv:0806.2807](#)].
- [110] J. Isern *et al.*, *J. Phys. Conf. Ser.* **172**, 012005 (2009), [[arXiv:0812.3043](#)].
- [111] A. Drlica-Wagner *et al.* (LSST Dark Matter Group) (2019), [[arXiv:1902.01055](#)].
- [112] J. Isern *et al.*, *Astron. & Astrophys.* **512**, A86 (2010).
- [113] A. H. Corsico *et al.*, *Mon. Not. Roy. Astron. Soc.* **424**, 2792 (2012), [[arXiv:1205.6180](#)].
- [114] A. H. Corsico *et al.*, *JCAP* **1212**, 010 (2012), [[arXiv:1211.3389](#)].
- [115] A. H. Córscico *et al.* (2019), [[arXiv:1907.00115](#)].
- [116] M. Giannotti *et al.*, *JCAP* **1605**, 05, 057 (2016), [[arXiv:1512.08108](#)].
- [117] G.G. Raffelt, *Stars as Laboratories for Fundamental Physics*, (Univ. of Chicago Press, Chicago, 1996).
- [118] T. Fischer *et al.*, *Phys. Rev. D* **94**, 8, 085012 (2016), [[arXiv:1605.08780](#)].
- [119] J. H. Chang, R. Essig and S. D. McDermott, *JHEP* **09**, 051 (2018), [[arXiv:1803.00993](#)].
- [120] P. Carenza *et al.*, *JCAP* **10**, 10, 016 (2019), [Erratum: *JCAP* 05, E01 (2020)], [[arXiv:1906.11844](#)].
- [121] M. S. Turner, *Phys. Rev. D* **45**, 1066 (1992).
- [122] G. Raffelt and D. Seckel, *Phys. Rev. D* **52**, 1780 (1995), [[arXiv:astro-ph/9312019](#)].
- [123] W. Keil *et al.*, *Phys. Rev. D* **56**, 2419 (1997), [[arXiv:astro-ph/9612222](#)].
- [124] B. Fore and S. Reddy, *Phys. Rev. C* **101**, 3, 035809 (2020), [[arXiv:1911.02632](#)].
- [125] P. Carenza *et al.*, *Phys. Rev. Lett.* **126**, 7, 071102 (2021), [[arXiv:2010.02943](#)].
- [126] J. Engel, D. Seckel and A. C. Hayes, *Phys. Rev. Lett.* **65**, 960 (1990).

- [127] T. Moroi and H. Murayama, *Phys. Lett.* **B440**, 69 (1998), [[hep-ph/9804291](#)].
- [128] D. Page *et al.*, *Phys. Rev. Lett.* **106**, 081101 (2011), [[arXiv:1011.6142](#)].
- [129] P. S. Shternin *et al.*, *Mon. Not. Roy. Astron. Soc.* **412**, L108 (2011), [[arXiv:1012.0045](#)].
- [130] L. B. Leinson, *Phys. Lett.* **B741**, 87 (2015), [[arXiv:1411.6833](#)].
- [131] K. Hamaguchi *et al.*, *Phys. Rev.* **D98**, 10, 103015 (2018), [[arXiv:1806.07151](#)].
- [132] J. Keller and A. Sedrakian, *Nucl. Phys.* **A897**, 62 (2013), [[arXiv:1205.6940](#)].
- [133] A. Sedrakian, *Phys. Rev.* **D93**, 6, 065044 (2016), [[arXiv:1512.07828](#)].
- [134] L. B. Leinson (2021), [[arXiv:2105.14745](#)].
- [135] L. B. Leinson, *JCAP* **1408**, 031 (2014), [[arXiv:1405.6873](#)].
- [136] B. Posselt and G. G. Pavlov, *Astrophys. J.* **864**, 2, 135 (2018), [[arXiv:1808.00531](#)].
- [137] M. V. Beznogov *et al.*, *Phys. Rev.* **C98**, 3, 035802 (2018), [[arXiv:1806.07991](#)].
- [138] P. W. Graham and S. Rajendran, *Phys. Rev.* **D88**, 035023 (2013), [[arXiv:1306.6088](#)].
- [139] G. G. Raffelt, J. Redondo and N. Viaux Maira, *Phys. Rev.* **D84**, 103008 (2011), [[arXiv:1110.6397](#)].
- [140] K. van Bibber *et al.*, *Phys. Rev.* **D39**, 2089 (1989).
- [141] D. M. Lazarus *et al.*, *Phys. Rev. Lett.* **69**, 2333 (1992).
- [142] S. Moriyama *et al.*, *Phys. Lett.* **B434**, 147 (1998), [[hep-ex/9805026](#)].
- [143] Y. Inoue *et al.*, *Phys. Lett.* **B536**, 18 (2002), [[arXiv:astro-ph/0204388](#)].
- [144] Y. Inoue *et al.*, *Phys. Lett.* **B668**, 93 (2008), [[arXiv:0806.2230](#)].
- [145] V. Anastassopoulos *et al.* (CAST), *Nature Phys.* **13**, 584 (2017), [[arXiv:1705.02290](#)].
- [146] E. Arik *et al.* (CAST), *JCAP* **0902**, 008 (2009), [[arXiv:0810.4482](#)].
- [147] S. Aune *et al.* (CAST), *Phys. Rev. Lett.* **107**, 261302 (2011), [[arXiv:1106.3919](#)].
- [148] M. Arik *et al.* (CAST), *Phys. Rev. Lett.* **112**, 9, 091302 (2014), [[arXiv:1307.1985](#)].
- [149] M. Arik *et al.* (CAST), *Phys. Rev.* **D92**, 2, 021101 (2015), [[arXiv:1503.00610](#)].
- [150] E. Armengaud *et al.*, *JINST* **9**, T05002 (2014), [[arXiv:1401.3233](#)].
- [151] E. Armengaud *et al.* (IAXO), *JCAP* **1906**, 06, 047 (2019), [[arXiv:1904.09155](#)].
- [152] M. Giannotti *et al.*, *JCAP* **1710**, 10, 010 (2017), [[arXiv:1708.02111](#)].
- [153] K. Barth *et al.*, *JCAP* **1305**, 010 (2013), [[arXiv:1302.6283](#)].
- [154] A. Abeln *et al.* (BabyIAXO), *JCAP* **2105**, 05, 137 (2021), [[arXiv:2010.12076](#)].
- [155] F. T. Avignone, III *et al.* (SOLAX), *Phys. Rev. Lett.* **81**, 5068 (1998), [[arXiv:astro-ph/9708008](#)].
- [156] S. Cebrian *et al.*, *Astropart. Phys.* **10**, 397 (1999), [[arXiv:astro-ph/9811359](#)].
- [157] A. Morales *et al.* (COSME), *Astropart. Phys.* **16**, 325 (2002), [[hep-ex/0101037](#)].
- [158] R. Bernabei *et al.*, *Phys. Lett.* **B515**, 6 (2001).
- [159] Z. Ahmed *et al.* (CDMS), *Phys. Rev. Lett.* **103**, 141802 (2009), [[arXiv:0902.4693](#)].
- [160] D. S. Akerib *et al.* (LUX), *Phys. Rev. Lett.* **118**, 26, 261301 (2017), [[arXiv:1704.02297](#)].
- [161] X. Zhou *et al.* (PandaX-II) (2020), [[arXiv:2008.06485](#)].
- [162] E. Aprile *et al.* (XENON), *Phys. Rev. D* **102**, 7, 072004 (2020), [[arXiv:2006.09721](#)].
- [163] L. Di Luzio *et al.*, *Phys. Rev. Lett.* **125**, 13, 131804 (2020), [[arXiv:2006.12487](#)].
- [164] C. Gao *et al.*, *Phys. Rev. Lett.* **125**, 13, 131806 (2020), [[arXiv:2006.14598](#)].

- [165] J. B. Dent *et al.*, Phys. Rev. Lett. **125**, 13, 131805 (2020), [arXiv:2006.15118].
- [166] J. W. Brockway, E. D. Carlson and G. G. Raffelt, Phys. Lett. **B383**, 439 (1996), [arXiv:astro-ph/9605197].
- [167] J. A. Grifols, E. Masso and R. Toldra, Phys. Rev. Lett. **77**, 2372 (1996), [arXiv:astro-ph/9606028].
- [168] A. Payez *et al.*, JCAP **1502**, 02, 006 (2015), [arXiv:1410.3747].
- [169] M. Meyer and T. Petrushevska, Phys. Rev. Lett. **124**, 23, 231101 (2020), [Erratum: Phys.Rev.Lett. 125, 119901 (2020)], [arXiv:2006.06722].
- [170] F. Calore *et al.*, Phys. Rev. D **102**, 12, 123005 (2020), [arXiv:2008.11741].
- [171] C. Dessert, J. W. Foster and B. R. Safdi, Phys. Rev. Lett. **125**, 26, 261102 (2020), [arXiv:2008.03305].
- [172] M. Xiao *et al.*, Phys. Rev. Lett. **126**, 3, 031101 (2021), [arXiv:2009.09059].
- [173] C. Dessert, J. W. Foster and B. R. Safdi, Astrophys. J. **904**, 1, 42 (2020), [arXiv:1910.02956].
- [174] M. Buschmann *et al.*, Phys. Rev. Lett. **126**, 2, 021102 (2021), [arXiv:1910.04164].
- [175] C. Dessert, A. J. Long and B. R. Safdi, Phys. Rev. Lett. **123**, 6, 061104 (2019), [arXiv:1903.05088].
- [176] C. Dessert, A. J. Long and B. R. Safdi (2021), [arXiv:2104.12772].
- [177] C. Csaki, N. Kaloper and J. Terning, Phys. Rev. Lett. **88**, 161302 (2002), [hep-ph/0111311].
- [178] A. Mirizzi, G.G. Raffelt, and P.D. Serpico, Lect. Notes Phys. **741**, 115 (2008).
- [179] R. Gill and J. S. Heyl, Phys. Rev. **D84**, 085001 (2011), [arXiv:1105.2083].
- [180] D. Horns *et al.*, Phys. Rev. **D85**, 085021 (2012), [arXiv:1203.2184].
- [181] A. Payez, J. R. Cudell and D. Hutzemeiers, JCAP **1207**, 041 (2012), [arXiv:1204.6187].
- [182] A. Dominguez, M. A. Sanchez-Conde and F. Prada, JCAP **1111**, 020 (2011), [arXiv:1106.1860].
- [183] W. Essey and A. Kusenko, Astrophys. J. **751**, L11 (2012), [arXiv:1111.0815].
- [184] D. Horns and M. Meyer, JCAP **1202**, 033 (2012), [arXiv:1201.4711].
- [185] G. I. Rubtsov and S. V. Troitsky, JETP Lett. **100**, 6, 355 (2014), [Pisma Zh. Eksp. Teor. Fiz.100,no.6,397(2014)], [arXiv:1406.0239].
- [186] K. Kohri and H. Kodama, Phys. Rev. **D96**, 5, 051701 (2017), [arXiv:1704.05189].
- [187] D. A. Sanchez, S. Fegan and B. Giebels, Astron. Astrophys. **554**, A75 (2013), [arXiv:1303.5923].
- [188] J. Biteau and D. A. Williams, Astrophys. J. **812**, 1, 60 (2015), [arXiv:1502.04166].
- [189] A. Domínguez and M. Ajello, Astrophys. J. **813**, 2, L34 (2015), [arXiv:1510.07913].
- [190] A. Korochkin, G. Rubtsov and S. Troitsky, JCAP **12**, 002 (2019), [arXiv:1810.03443].
- [191] A. De Angelis, G. Galanti and M. Roncadelli, Phys. Rev. **D84**, 105030 (2011), [Erratum: Phys. Rev.D87,no.10,109903(2013)], [arXiv:1106.1132].
- [192] M. Simet, D. Hooper and P. D. Serpico, Phys. Rev. **D77**, 063001 (2008), [arXiv:0712.2825].
- [193] M. A. Sanchez-Conde *et al.*, Phys. Rev. **D79**, 123511 (2009), [arXiv:0905.3270].
- [194] M. Meyer, D. Horns and M. Raue, Phys. Rev. **D87**, 3, 035027 (2013), [arXiv:1302.1208].
- [195] A. Abramowski *et al.* (H.E.S.S.), Phys. Rev. **D88**, 10, 102003 (2013), [arXiv:1311.3148].
- [196] M. Ajello *et al.* (Fermi-LAT), Phys. Rev. Lett. **116**, 16, 161101 (2016), [arXiv:1603.06978].

- [197] C. Zhang *et al.*, Phys. Rev. **D97**, 6, 063009 (2018), [arXiv:1802.08420].
- [198] H.-J. Li *et al.*, Phys. Rev. D **103**, 8, 083003 (2021), [arXiv:2008.09464].
- [199] M. Libanov and S. Troitsky, Phys. Lett. B **802**, 135252 (2020), [arXiv:1908.03084].
- [200] Z.-Q. Xia *et al.*, Phys. Rev. **D97**, 6, 063003 (2018), [arXiv:1801.01646].
- [201] J. Majumdar, F. Calore and D. Horns, JCAP **1804**, 04, 048 (2018), [arXiv:1801.08813].
- [202] G. A. Pallathadka *et al.* (2020), [arXiv:2008.08100].
- [203] K. Choi *et al.*, Phys. Rev. D **101**, 4, 043007 (2020), [arXiv:1806.09508].
- [204] F. Chadha-Day (2021), [arXiv:2107.12813].
- [205] D. Wouters and P. Brun, Astrophys. J. **772**, 44 (2013), [arXiv:1304.0989].
- [206] M. Berg *et al.*, Astrophys. J. **847**, 2, 101 (2017), [arXiv:1605.01043].
- [207] M. C. D. Marsh *et al.*, JCAP **1712**, 12, 036 (2017), [arXiv:1703.07354].
- [208] J. P. Conlon *et al.*, JCAP **1707**, 07, 005 (2017), [arXiv:1704.05256].
- [209] L. Chen and J. P. Conlon, Mon. Not. Roy. Astron. Soc. **479**, 2, 2243 (2018), [arXiv:1712.08313].
- [210] C. S. Reynolds *et al.*, Astrophys. J. **890**, 1, 59 (2020), [arXiv:1907.05475].
- [211] A. Hook and J. Huang, JHEP **06**, 036 (2018), [arXiv:1708.08464].
- [212] J. Huang *et al.*, Phys. Rev. D **99**, 6, 063013 (2019), [arXiv:1807.02133].
- [213] J. Zhang *et al.* (2021), [arXiv:2105.13963].
- [214] G. Bellini *et al.* (Borexino), Phys. Rev. D **89**, 11, 112007 (2014), [arXiv:1308.0443].
- [215] B. P. Abbott *et al.* (LIGO Scientific, Virgo), Phys. Rev. Lett. **119**, 16, 161101 (2017), [arXiv:1710.05832].
- [216] A. Arvanitaki and S. Dubovsky, Phys. Rev. **D83**, 044026 (2011), [arXiv:1004.3558].
- [217] A. Arvanitaki, M. Baryakhtar and X. Huang, Phys. Rev. **D91**, 8, 084011 (2015), [arXiv:1411.2263].
- [218] V. M. Mehta *et al.* (2020), [arXiv:2011.08693].
- [219] V. M. Mehta *et al.*, JCAP **07**, 033 (2021), [arXiv:2103.06812].
- [220] M. J. Stott (2020), [arXiv:2009.07206].
- [221] M. Baryakhtar *et al.*, Phys. Rev. D **103**, 9, 095019 (2021), [arXiv:2011.11646].
- [222] A. Arvanitaki *et al.*, Phys. Rev. **D95**, 4, 043001 (2017), [arXiv:1604.03958].
- [223] K. K. Y. Ng *et al.*, Phys. Rev. D **103**, 6, 063010 (2021), [arXiv:1908.02312].
- [224] E. Masso, F. Rota and G. Zsembinszki, Phys. Rev. D **66**, 023004 (2002), [hep-ph/0203221].
- [225] P. Graf and F. D. Steffen, Phys. Rev. D **83**, 075011 (2011), [arXiv:1008.4528].
- [226] Z. G. Berezhiani, A. S. Sakharov and M. Y. Khlopov, Sov. J. Nucl. Phys. **55**, 1063 (1992).
- [227] S. Hannestad, A. Mirizzi and G. Raffelt, JCAP **07**, 002 (2005), [hep-ph/0504059].
- [228] S. Hannestad *et al.*, JCAP **08**, 001 (2010), [arXiv:1004.0695].
- [229] M. Archidiacono *et al.*, JCAP **10**, 020 (2013), [arXiv:1307.0615].
- [230] E. Di Valentino *et al.*, Phys. Lett. B **752**, 182 (2016), [arXiv:1507.08665].
- [231] W. Giarè *et al.*, Mon. Not. Roy. Astron. Soc. **505**, 2, 2703 (2021), [arXiv:2011.14704].
- [232] L. Di Luzio, G. Martinelli and G. Piazza, Phys. Rev. Lett. **126**, 24, 241801 (2021), [arXiv:2101.10330].

- [233] E. Masso and R. Toldra, *Phys. Rev. D* **52**, 1755 (1995), [[hep-ph/9503293](#)].
- [234] E. Masso and R. Toldra, *Phys. Rev. D* **55**, 7967 (1997), [[hep-ph/9702275](#)].
- [235] D. Cadamuro and J. Redondo, *JCAP* **1202**, 032 (2012), [[arXiv:1110.2895](#)].
- [236] P. F. Depta, M. Hufnagel and K. Schmidt-Hoberg, *JCAP* **05**, 009 (2020), [[arXiv:2002.08370](#)].
- [237] J. Preskill, M. B. Wise and F. Wilczek, *Phys. Lett. B* **120**, 127 (1983).
- [238] L. F. Abbott and P. Sikivie, *Phys. Lett. B* **120**, 133 (1983).
- [239] M. Dine and W. Fischler, *Phys. Lett. B* **120**, 137 (1983).
- [240] K. J. Bae, J.-H. Huh and J. E. Kim, *JCAP* **0809**, 005 (2008), [[arXiv:0806.0497](#)].
- [241] O. Wantz and E. P. S. Shellard, *Phys. Rev. D* **82**, 123508 (2010), [[arXiv:0910.1066](#)].
- [242] G. Ballesteros *et al.*, *JCAP* **1708**, 08, 001 (2017), [[arXiv:1610.01639](#)].
- [243] R. T. Co, F. D'Eramo and L. J. Hall, *Phys. Rev. D* **94**, 7, 075001 (2016), [[arXiv:1603.04439](#)].
- [244] M. Tegmark *et al.*, *Phys. Rev. D* **73**, 023505 (2006), [[arXiv:astro-ph/0511774](#)].
- [245] A. D. Linde, *Phys. Lett. 158B*, 375 (1985).
- [246] D. Seckel and M. S. Turner, *Phys. Rev. D* **32**, 3178 (1985).
- [247] M. Beltran, J. Garcia-Bellido and J. Lesgourges, *Phys. Rev. D* **75**, 103507 (2007), [[hep-ph/0606107](#)].
- [248] M. P. Hertzberg, M. Tegmark and F. Wilczek, *Phys. Rev. D* **78**, 083507 (2008), [[arXiv:0807.1726](#)].
- [249] J. Hamann *et al.*, *JCAP* **0906**, 022 (2009), [[arXiv:0904.0647](#)].
- [250] P. A. R. Ade *et al.* (Planck), *Astron. Astrophys.* **571**, A22 (2014), [[arXiv:1303.5082](#)].
- [251] P. A. R. Ade *et al.* (Planck), *Astron. Astrophys.* **594**, A20 (2016), [[arXiv:1502.02114](#)].
- [252] R. T. Co, L. J. Hall and K. Harigaya, *Phys. Rev. Lett.* **124**, 25, 251802 (2020), [[arXiv:1910.14152](#)].
- [253] S. Chang, C. Hagmann and P. Sikivie, *Phys. Rev. D* **59**, 023505 (1999), [[hep-ph/9807374](#)].
- [254] C. Hagmann, S. Chang and P. Sikivie, *Phys. Rev. D* **63**, 125018 (2001), [[hep-ph/0012361](#)].
- [255] T. Hiramatsu *et al.*, *Phys. Rev. D* **83**, 123531 (2011), [[arXiv:1012.5502](#)].
- [256] T. Hiramatsu *et al.*, *Phys. Rev. D* **85**, 105020 (2012), [Erratum: *Phys. Rev.D86,089902(2012)*], [[arXiv:1202.5851](#)].
- [257] M. Kawasaki, K. Saikawa and T. Sekiguchi, *Phys. Rev. D* **91**, 6, 065014 (2015), [[arXiv:1412.0789](#)].
- [258] V. B. Klaer and G. D. Moore, *JCAP* **1711**, 11, 049 (2017), [[arXiv:1708.07521](#)].
- [259] M. Gorgetto, E. Hardy and G. Villadoro, *JHEP* **07**, 151 (2018), [[arXiv:1806.04677](#)].
- [260] M. Buschmann, J. W. Foster and B. R. Safdi, *Phys. Rev. Lett.* **124**, 16, 161103 (2020), [[arXiv:1906.00967](#)].
- [261] M. Hindmarsh *et al.*, *Phys. Rev. Lett.* **124**, 2, 021301 (2020), [[arXiv:1908.03522](#)].
- [262] M. Gorgetto, E. Hardy and G. Villadoro, *SciPost Phys.* **10**, 050 (2021), [[arXiv:2007.04990](#)].
- [263] M. Dine *et al.* (2020), [[arXiv:2012.13065](#)].
- [264] M. Hindmarsh *et al.*, *Phys. Rev. D* **103**, 10, 103534 (2021), [[arXiv:2102.07723](#)].
- [265] M. Buschmann *et al.* (2021), [[arXiv:2108.05368](#)].
- [266] A. Ringwald and K. Saikawa, *Phys. Rev. D* **93**, 8, 085031 (2016), [Addendum: *Phys. Rev.D94,no.4,049908(2016)*], [[arXiv:1512.06436](#)].

- [267] T. Hiramatsu *et al.*, *JCAP* **1301**, 001 (2013), [[arXiv:1207.3166](#)].
- [268] C. J. Hogan and M. J. Rees, *Phys. Lett.* **B205**, 228 (1988).
- [269] E. W. Kolb and I. I. Tkachev, *Phys. Rev. Lett.* **71**, 3051 (1993), [[hep-ph/9303313](#)].
- [270] B. Eggemeier *et al.*, *Phys. Rev. Lett.* **125**, 4, 041301 (2020), [[arXiv:1911.09417](#)].
- [271] A. Vaquero, J. Redondo and J. Stadler (2018), [*JCAP*1904,no.04,012(2019)], [[arXiv:1809.09241](#)].
- [272] E. W. Kolb and I. I. Tkachev, *Astrophys. J.* **460**, L25 (1996), [[arXiv:astro-ph/9510043](#)].
- [273] M. Fairbairn, D. J. E. Marsh and J. Quevillon, *Phys. Rev. Lett.* **119**, 2, 021101 (2017), [[arXiv:1701.04787](#)].
- [274] A. Katz *et al.*, *JCAP* **1812**, 005 (2018), [[arXiv:1807.11495](#)].
- [275] E. Berkowitz, M. I. Buchoff and E. Rinaldi, *Phys. Rev.* **D92**, 3, 034507 (2015), [[arXiv:1505.07455](#)].
- [276] S. Borsanyi *et al.*, *Phys. Lett.* **B752**, 175 (2016), [[arXiv:1508.06917](#)].
- [277] R. Kitano and N. Yamada, *JHEP* **10**, 136 (2015), [[arXiv:1506.00370](#)].
- [278] P. Petreczky, H.-P. Schadler and S. Sharma, *Phys. Lett.* **B762**, 498 (2016), [[arXiv:1606.03145](#)].
- [279] Y. Taniguchi *et al.*, *Phys. Rev.* **D95**, 5, 054502 (2017), [[arXiv:1611.02411](#)].
- [280] M. Dine *et al.*, *Phys. Rev.* **D96**, 9, 095001 (2017), [[arXiv:1705.00676](#)].
- [281] R. D. Pisarski and L. G. Yaffe, *Phys. Lett.* **97B**, 110 (1980).
- [282] R. Hlozek *et al.*, *Phys. Rev.* **D91**, 10, 103512 (2015), [[arXiv:1410.2896](#)].
- [283] D. J. E. Marsh, *Phys. Rept.* **643**, 1 (2016), [[arXiv:1510.07633](#)].
- [284] L. Hui *et al.*, *Phys. Rev.* **D95**, 4, 043541 (2017), [[arXiv:1610.08297](#)].
- [285] G. P. Centers *et al.* (2019), [[arXiv:1905.13650](#)].
- [286] A. G. Dias *et al.*, *JHEP* **06**, 037 (2014), [[arXiv:1403.5760](#)].
- [287] J. E. Kim and D. J. E. Marsh, *Phys. Rev.* **D93**, 2, 025027 (2016), [[arXiv:1510.01701](#)].
- [288] H. Davoudiasl and C. W. Murphy, *Phys. Rev. Lett.* **118**, 14, 141801 (2017), [[arXiv:1701.01136](#)].
- [289] L. Di Luzio *et al.*, *JCAP* **10**, 001 (2021), [[arXiv:2102.01082](#)].
- [290] M. Khlopov, B. A. Malomed and I. B. Zeldovich, *Mon. Not. Roy. Astron. Soc.* **215**, 575 (1985).
- [291] W. Hu, R. Barkana and A. Gruzinov, *Phys. Rev. Lett.* **85**, 1158 (2000), [[arXiv:astro-ph/0003365](#)].
- [292] L. Amendola and R. Barbieri, *Phys. Lett.* **B642**, 192 (2006), [[hep-ph/0509257](#)].
- [293] D. J. E. Marsh and P. G. Ferreira, *Phys. Rev.* **D82**, 103528 (2010), [[arXiv:1009.3501](#)].
- [294] E. Seidel and W. M. Suen, *Phys. Rev. Lett.* **66**, 1659 (1991).
- [295] H.-Y. Schive, T. Chiueh and T. Broadhurst, *Nature Phys.* **10**, 496 (2014), [[arXiv:1406.6586](#)].
- [296] D. G. Levkov, A. G. Panin and I. I. Tkachev, *Phys. Rev. Lett.* **121**, 15, 151301 (2018), [[arXiv:1804.05857](#)].
- [297] B. Eggemeier and J. C. Niemeyer, *Phys. Rev. D* **100**, 6, 063528 (2019), [[arXiv:1906.01348](#)].
- [298] R. Hlozek, D. J. E. Marsh and D. Grin, *Mon. Not. Roy. Astron. Soc.* **476**, 3, 3063 (2018), [[arXiv:1708.05681](#)].

- [299] D. J. E. Marsh and J. Silk, *Mon. Not. Roy. Astron. Soc.* **437**, 3, 2652 (2014), [[arXiv:1307.1705](#)].
- [300] H.-Y. Schive *et al.*, *Astrophys. J.* **818**, 1, 89 (2016), [[arXiv:1508.04621](#)].
- [301] B. Bozek *et al.*, *Mon. Not. Roy. Astron. Soc.* **450**, 1, 209 (2015), [[arXiv:1409.3544](#)].
- [302] P. S. Corasaniti *et al.*, *Phys. Rev.* **D95**, 8, 083512 (2017), [[arXiv:1611.05892](#)].
- [303] K. K. Rogers and H. V. Peiris, *Phys. Rev. Lett.* **126**, 7, 071302 (2021), [[arXiv:2007.12705](#)].
- [304] H.-Y. Schive and T. Chiueh, *Mon. Not. Roy. Astron. Soc.* **473**, 1, L36 (2018), [[arXiv:1706.03723](#)].
- [305] E. O. Nadler *et al.* (DES), *Phys. Rev. Lett.* **126**, 091101 (2021), [[arXiv:2008.00022](#)].
- [306] B. Schwabe, J. C. Niemeyer and J. F. Engels, *Phys. Rev.* **D94**, 4, 043513 (2016), [[arXiv:1606.05151](#)].
- [307] J. Veltmaat and J. C. Niemeyer, *Phys. Rev.* **D94**, 12, 123523 (2016), [[arXiv:1608.00802](#)].
- [308] P. Mocz *et al.*, *Mon. Not. Roy. Astron. Soc.* **471**, 4, 4559 (2017), [[arXiv:1705.05845](#)].
- [309] D. G. Levkov, A. G. Panin and I. I. Tkachev, *Phys. Rev. Lett.* **118**, 011301 (2017); T. Helfer *et al.*, *JCAP* **1703**, 03, 055 (2017), [[arXiv:1609.04724](#)].
- [310] D. J. E. Marsh and A.-R. Pop, *Mon. Not. Roy. Astron. Soc.* **451**, 3, 2479 (2015), [[arXiv:1502.03456](#)].
- [311] S.-R. Chen, H.-Y. Schive and T. Chiueh, *Mon. Not. Roy. Astron. Soc.* **468**, 2, 1338 (2017), [[arXiv:1606.09030](#)].
- [312] A. X. González-Morales *et al.*, *Mon. Not. Roy. Astron. Soc.* **472**, 2, 1346 (2017), [[arXiv:1609.05856](#)].
- [313] I. De Martino *et al.*, *Phys. Dark Univ.* **28**, 100503 (2020), [[arXiv:1807.08153](#)].
- [314] T. Broadhurst *et al.*, *Phys. Rev. D* **101**, 8, 083012 (2020), [[arXiv:1902.10488](#)].
- [315] H.-Y. Schive *et al.*, *Phys. Rev. Lett.* **113**, 26, 261302 (2014), [[arXiv:1407.7762](#)].
- [316] V. H. Robles, J. S. Bullock and M. Boylan-Kolchin, *Mon. Not. Roy. Astron. Soc.* **483**, 1, 289 (2019), [[arXiv:1807.06018](#)].
- [317] V. Desjacques and A. Nusser (2019), [[arXiv:1905.03450](#)].
- [318] M. Safarzadeh and D. N. Spergel (2019), [[arXiv:1906.11848](#)].
- [319] A. Pontzen and F. Governato, *Nature* **506**, 171 (2014), [[arXiv:1402.1764](#)].
- [320] P. Mocz *et al.*, *Phys. Rev. Lett.* **123**, 14, 141301 (2019), [[arXiv:1910.01653](#)].
- [321] J. Veltmaat, B. Schwabe and J. C. Niemeyer, *Phys. Rev. D* **101**, 8, 083518 (2020), [[arXiv:1911.09614](#)].
- [322] J. Veltmaat, J. C. Niemeyer and B. Schwabe, *Phys. Rev.* **D98**, 4, 043509 (2018), [[arXiv:1804.09647](#)].
- [323] B. Bar-Or, J.-B. Fouvry and S. Tremaine, *Astrophys. J.* **871**, 1, 28 (2019), [[arXiv:1809.07673](#)].
- [324] B. V. Church, P. Mocz and J. P. Ostriker, *MNRAS* **485**, 2861 (2019), [[arXiv:1809.04744](#)].
- [325] N. C. Amorisco and A. Loeb (2018), [[arXiv:1808.00464](#)].
- [326] T. S. Li *et al.* (DES), *Astrophys. J.* **838**, 1, 8 (2017), [[arXiv:1611.05052](#)].
- [327] D. J. E. Marsh and J. C. Niemeyer, *Phys. Rev. Lett.* **123**, 5, 051103 (2019), [[arXiv:1810.08543](#)].
- [328] E. Armengaud *et al.* (EDELWEISS), *Phys. Rev. D* **98**, 8, 082004 (2018), [[arXiv:1808.02340](#)].

- [329] C. Fu *et al.* (PandaX), Phys. Rev. Lett. **119**, 18, 181806 (2017), [[arXiv:1707.07921](#)].
- [330] T. Aralis *et al.* (SuperCDMS), Phys. Rev. D **101**, 5, 052008 (2020), [Erratum: Phys. Rev. D **103**, 039901 (2021)], [[arXiv:1911.11905](#)].
- [331] E. Aprile *et al.* (XENON), Phys. Rev. Lett. **123**, 25, 251801 (2019), [[arXiv:1907.11485](#)].
- [332] M. Regis *et al.*, Phys. Lett. B **814**, 136075 (2021), [[arXiv:2009.01310](#)].
- [333] B. D. Blout *et al.*, Astrophys. J. **546**, 825 (2001), [[arXiv:astro-ph/0006310](#)].
- [334] K. Kelley and P. J. Quinn, Astrophys. J. **845**, 1, L4 (2017), [[arXiv:1708.01399](#)].
- [335] G. Sigl, Phys. Rev. **D96**, 10, 103014 (2017), [[arXiv:1708.08908](#)].
- [336] A. Hook *et al.*, Phys. Rev. Lett. **121**, 24, 241102 (2018), [[arXiv:1804.03145](#)].
- [337] J. W. Foster *et al.*, Phys. Rev. Lett. **125**, 17, 171301 (2020), [[arXiv:2004.00011](#)].
- [338] J. Darling, Astrophys. J. Lett. **900**, 2, L28 (2020), [[arXiv:2008.11188](#)].
- [339] R. A. Battye *et al.* (2021), [[arXiv:2107.01225](#)].
- [340] S. J. Witte *et al.* (2021), [[arXiv:2104.07670](#)].
- [341] R. A. Battye *et al.* (2021), [[arXiv:2104.08290](#)].
- [342] A. J. Millar *et al.* (2021), [[arXiv:2107.07399](#)].
- [343] A. Caputo *et al.*, JCAP **1903**, 03, 027 (2019), [[arXiv:1811.08436](#)].
- [344] P. Carenza, A. Mirizzi and G. Sigl, Phys. Rev. D **101**, 10, 103016 (2020), [[arXiv:1911.07838](#)].
- [345] D. G. Levkov, A. G. Panin and I. I. Tkachev, Phys. Rev. D **102**, 2, 023501 (2020), [[arXiv:2004.05179](#)].
- [346] M. A. Fedderke, P. W. Graham and S. Rajendran, Phys. Rev. **D100**, 1, 015040 (2019), [[arXiv:1903.02666](#)].
- [347] T. Fujita *et al.*, Phys. Rev. D **103**, 4, 043509 (2021), [[arXiv:2011.11894](#)].
- [348] P. A. R. Ade *et al.* (BICEP/Keck) (2021), [[arXiv:2108.03316](#)].
- [349] T. Liu, G. Smoot and Y. Zhao (2019), [[arXiv:1901.10981](#)].
- [350] P. Sikivie, Phys. Rev. **D32**, 2988 (1985), [Erratum: Phys. Rev. D36, 974 (1987)].
- [351] R. Bradley *et al.*, Rev. Mod. Phys. **75**, 777 (2003).
- [352] P. Sikivie and J. R. Ipser, Phys. Lett. **B291**, 288 (1992).
- [353] P. Sikivie, I. I. Tkachev and Y. Wang, Phys. Rev. Lett. **75**, 2911 (1995), [[arXiv:astro-ph/9504052](#)].
- [354] S. De Panfilis *et al.*, Phys. Rev. Lett. **59**, 839 (1987).
- [355] W. Wuensch *et al.*, Phys. Rev. **D40**, 3153 (1989).
- [356] C. Hagmann *et al.*, Phys. Rev. **D42**, 1297 (1990).
- [357] S. J. Asztalos *et al.* (ADMX), Phys. Rev. **D69**, 011101 (2004), [[arXiv:astro-ph/0310042](#)].
- [358] L. Duffy *et al.*, Phys. Rev. Lett. **95**, 091304 (2005), [[arXiv:astro-ph/0505237](#)]; J. Hoskins *et al.*, Phys. Rev. **D84**, 121302 (2011), [[arXiv:1109.4128](#)].
- [359] S. J. Asztalos *et al.* (ADMX), Phys. Rev. Lett. **104**, 041301 (2010), [[arXiv:0910.5914](#)].
- [360] S. J. Asztalos *et al.* (ADMX), Nucl. Instrum. Meth. **A656**, 39 (2011), [[arXiv:1105.4203](#)].
- [361] R. Khatiwada *et al.* (ADMX) (2020), [[arXiv:2010.00169](#)].
- [362] N. Du *et al.* (ADMX), Phys. Rev. Lett. **120**, 15, 151301 (2018), [[arXiv:1804.05750](#)].
- [363] T. Braine *et al.* (ADMX), Phys. Rev. Lett. **124**, 10, 101303 (2020), [[arXiv:1910.08638](#)].

- [364] C. Bartram *et al.* (ADMX), *Phys. Rev. D* **103**, 3, 032002 (2021), [[arXiv:2010.06183](#)].
- [365] G. Rybka *et al.* (ADMX), *Phys. Rev. Lett.* **105**, 051801 (2010), [[arXiv:1004.5160](#)].
- [366] A. Wagner *et al.* (ADMX), *Phys. Rev. Lett.* **105**, 171801 (2010), [[arXiv:1007.3766](#)].
- [367] C. Boutan *et al.* (ADMX), *Phys. Rev. Lett.* **121**, 26, 261302 (2018), [[arXiv:1901.00920](#)].
- [368] B. M. Brubaker *et al.*, *Phys. Rev. Lett.* **118**, 6, 061302 (2017), [[arXiv:1610.02580](#)].
- [369] L. Zhong *et al.* (HAYSTAC), *Phys. Rev. D* **97**, 9, 092001 (2018), [[arXiv:1803.03690](#)].
- [370] K. M. Backes *et al.* (HAYSTAC), *Nature* **590**, 7845, 238 (2021), [[arXiv:2008.01853](#)].
- [371] B. T. McAllister *et al.*, *Phys. Dark Univ.* **18**, 67 (2017), [[arXiv:1706.00209](#)].
- [372] D. Alesini *et al.*, *Phys. Rev. D* **99**, 10, 101101 (2019), [[arXiv:1903.06547](#)].
- [373] D. Alesini *et al.*, *Phys. Rev. D* **103**, 10, 102004 (2021), [[arXiv:2012.09498](#)].
- [374] A. A. Melcón *et al.* (CAST) (2021), [[arXiv:2104.13798](#)].
- [375] S. Lee *et al.*, *Phys. Rev. Lett.* **124**, 10, 101802 (2020), [[arXiv:2001.05102](#)].
- [376] J. Jeong *et al.*, *Phys. Rev. Lett.* **125**, 22, 221302 (2020), [[arXiv:2008.10141](#)].
- [377] O. Kwon *et al.* (CAPP), *Phys. Rev. Lett.* **126**, 19, 191802 (2021), [[arXiv:2012.10764](#)].
- [378] G. Rybka *et al.*, *Phys. Rev. D* **91**, 1, 011701 (2015), [[arXiv:1403.3121](#)].
- [379] M. Lawson *et al.*, *Phys. Rev. Lett.* **123**, 14, 141802 (2019), [[arXiv:1904.11872](#)].
- [380] D. Horns *et al.*, *JCAP* **1304**, 016 (2013), [[arXiv:1212.2970](#)].
- [381] A. Caldwell *et al.* (MADMAX Working Group), *Phys. Rev. Lett.* **118**, 9, 091801 (2017), [[arXiv:1611.05865](#)].
- [382] P. Brun *et al.* (MADMAX), *Eur. Phys. J.* **C79**, 3, 186 (2019), [[arXiv:1901.07401](#)].
- [383] M. Baryakhtar, J. Huang and R. Lasenby, *Phys. Rev. D* **98**, 3, 035006 (2018), [[arXiv:1803.11455](#)].
- [384] A. Arvanitaki, S. Dimopoulos and K. Van Tilburg, *Phys. Rev. X* **8**, 4, 041001 (2018), [[arXiv:1709.05354](#)].
- [385] C. A. Thomson *et al.*, *Phys. Rev. Lett.* **126**, 8, 081803 (2021), [Erratum: *Phys. Rev. Lett.* 127, 019901 (2021)], [[arXiv:1912.07751](#)].
- [386] A. Berlin *et al.*, *JHEP* **07**, 07, 088 (2020), [[arXiv:1912.11048](#)].
- [387] P. Sikivie, *Phys. Rev. Lett.* **113**, 20, 201301 (2014), [Erratum: *Phys. Rev. Lett.* 125, 029901 (2020)], [[arXiv:1409.2806](#)].
- [388] R. Li *et al.*, *Nature Phys.* **6**, 284 (2010), [[arXiv:0908.1537](#)].
- [389] K. Ishiwata, *Phys. Rev. D* **104**, 1, 016004 (2021), [[arXiv:2103.02848](#)].
- [390] L. Cao *et al.*, *Phys. Rev. B* **104**, 054421 (2021), URL <https://link.aps.org/doi/10.1103/PhysRevB.104.054421>.
- [391] D. J. E. Marsh *et al.*, *Phys. Rev. Lett.* **123**, 12, 121601 (2019), [[arXiv:1807.08810](#)].
- [392] J. Schütte-Engel *et al.*, *JCAP* **08**, 066 (2021), [[arXiv:2102.05366](#)].
- [393] P. Sikivie, N. Sullivan, and D. B. Tanner, *Phys. Rev. Lett.* **112**, 131301 (2014).
- [394] Y. Kahn, B. R. Safdi and J. Thaler, *Phys. Rev. Lett.* **117**, 14, 141801 (2016), [[arXiv:1602.01086](#)].
- [395] J. L. Ouellet *et al.* (ABRACADABRA), *Phys. Rev. Lett.* **122**, 12, 121802 (2019), [[arXiv:1810.12257](#)].
- [396] C. P. Salemi *et al.*, *Phys. Rev. Lett.* **127**, 8, 081801 (2021), [[arXiv:2102.06722](#)].

- [397] N. Crisosto *et al.*, Phys. Rev. Lett. **124**, 24, 241101 (2020), [arXiv:1911.05772].
- [398] A. V. Gramolin *et al.*, Nature Phys. **17**, 1, 79 (2021), [arXiv:2003.03348].
- [399] J. A. Devlin *et al.*, Phys. Rev. Lett. **126**, 4, 041301 (2021), [arXiv:2101.11290].
- [400] M. Silva-Feaver *et al.*, IEEE Trans. Appl. Supercond. **27**, 4, 1400204 (2017), [arXiv:1610.09344].
- [401] C. Abel *et al.*, Phys. Rev. **X7**, 4, 041034 (2017), [arXiv:1708.06367].
- [402] K. Blum *et al.*, Phys. Lett. B **737**, 30 (2014), [arXiv:1401.6460].
- [403] D. Budker *et al.*, Phys. Rev. **X4**, 2, 021030 (2014), [arXiv:1306.6089].
- [404] M. B. Wise, H. Georgi and S. L. Glashow, Phys. Rev. Lett. **47**, 402 (1981).
- [405] A. Ernst, A. Ringwald and C. Tamarit, JHEP **02**, 103 (2018), [arXiv:1801.04906].
- [406] L. Di Luzio, A. Ringwald and C. Tamarit, Phys. Rev. **D98**, 9, 095011 (2018), [arXiv:1807.09769].
- [407] P. Fileviez Perez, C. Murgui and A. D. Plascencia (2019), [arXiv:1908.01772].
- [408] D. Aybas *et al.*, Phys. Rev. Lett. **126**, 14, 141802 (2021), [arXiv:2101.01241].
- [409] T. Wu *et al.*, Phys. Rev. Lett. **122**, 19, 191302 (2019), [arXiv:1901.10843].
- [410] A. Garcon *et al.*, Sci. Adv. **5**, 10, eaax4539 (2019), [arXiv:1902.04644].
- [411] I. M. Bloch *et al.* (NASDUCK) (2021), [arXiv:2105.04603].
- [412] G. Vasilakis *et al.*, Physical Review Letters **103**, 26 (2009), ISSN 1079-7114, URL <http://dx.doi.org/10.1103/PhysRevLett.103.261801>.
- [413] I. M. Bloch *et al.*, JHEP **01**, 167 (2020), [arXiv:1907.03767].
- [414] S. P. Chang *et al.*, Phys. Rev. **D99**, 8, 083002 (2019), [arXiv:1710.05271].
- [415] L. Krauss *et al.*, Phys. Rev. Lett. **55**, 1797 (1985).
- [416] R. Barbieri *et al.*, Phys. Lett. B **226**, 357 (1989).
- [417] R. Barbieri *et al.*, Phys. Dark Univ. **15**, 135 (2017), [arXiv:1606.02201].
- [418] N. Crescini *et al.* (QUAX), Phys. Rev. Lett. **124**, 17, 171801 (2020), [arXiv:2001.08940].